

Demographic back-casting reveals that subtle
dimensions of climate change have strong effects
on population viability

Kevin Czachura and Tom E.X. Miller*

Program in Ecology and Evolutionary Biology, Department of
BioSciences, Rice University, Houston, TX USA

*Corresponding author: tom.miller@rice.edu (1-713-348-4218)

Abstract

- 1 1. The effects of climate change on population viability reflect the net influ-
2 ence of potentially diverse responses of individual-level demographic pro-
3 cesses (growth, survival, regeneration) to multiple components of climate.
4 Articulating climate-demography connections can facilitate forecasts of re-
5 sponses to future climate change as well as back-casts that may reveal how
6 populations responded to historical climate change.
- 7 2. We studied climate-demography relationships in the cactus *Cyclindriopun-*
8 *tia imbricata*; previous work indicated that our focal population has high
9 abundance but a negative population growth rate, where deaths exceed
10 births, suggesting that it persists under extinction debt. We parameter-
11 ized a climate-dependent integral projection model with data from a 14-year
12 field study, then back-casted expected population growth rates since 1900
13 to test the hypothesis that recent climate change has driven this population
14 into extinction debt.
- 15 3. We found clear patterns of climate change in our central New Mexico study
16 region but, contrary to our hypothesis, *C. imbricata* has most likely bene-
17 fitted from recent climate change and is on track to reach replacement-level
18 population growth within 37 years, or sooner if climate change accelerates.
19 Furthermore, the strongest feature of climate change (a trend toward years
20 that are overall warmer and drier, captured by the first principal component
21 of inter-annual variation) was not the main driver of population responses.
22 Instead, temporal trends in population growth were dominated by more sub-

23 tle, seasonal climatic factors with relatively weak signals of recent change
24 (wetter and milder cool seasons, captured by the second and third principal
25 components).

26 4. *Synthesis*. Our results highlight the challenges of **back-casting or** forecasting
27 population dynamics under climate change, since the most apparent features
28 of climate change may not be the most important drivers of ecological re-
29 sponses. Environmentally explicit demographic models can help meet this
30 challenge, but they must consider the magnitudes of different aspects of cli-
31 mate change alongside the magnitudes of demographic responses to those
32 changes.

33 Keywords

34 Cactaceae; Climate change; Demography; Extinction debt; Integral Projection
35 Model; Long-term ecological research

36 Introduction

37 Population extinction debt is likely to increase in frequency as a fingerprint of
38 global change, including climate change (Dullinger *et al.*, 2012; Urban, 2015). Ex-
39 tinction debt is a form of transient dynamics whereby populations persist despite
40 having population growth rates that fall below replacement level ($\lambda < 1$), suggest-
41 ing a long-term trajectory toward local extinction but with potentially long time
42 lags (Hastings *et al.*, 2018; Kuussaari *et al.*, 2009). While extinction debt is often
43 studied through species richness patterns at the community level (e.g., Vellend
44 *et al.* 2006), there is recent emphasis on the underlying single-species dynamics
45 whereby populations transition from positive to negative growth rates (Lehtilä
46 *et al.*, 2016; Hylander & Ehrlén, 2013). In the absence of significant migration
47 (which can maintain populations in sink habitats), extinction debt suggests that
48 the environment was more favorable for population growth at some time in the
49 past. However, the mechanisms that cause populations to tip from positive to
50 negative growth rates are rarely known, and this information may be critical for
51 effective conservation planning (Hylander & Ehrlén, 2013).

52 Structured population models built from individual-level demographic rates
53 provide a powerful framework for studying drivers of extinction debt (Lehtilä *et al.*,
54 2016) and environment-dependent population dynamics more generally (Ehrlén &
55 Morris, 2015). By incorporating climatic factors as statistical covariates, previ-
56 ous studies have identified climatic limits of population viability and forecasted
57 responses to particular types of climate change (e.g., Adler *et al.* 2013; Maschin-
58 ski *et al.* 2006; Jenouvrier *et al.* 2014). Additionally, articulating the connec-
59 tions between environment and demography can allow for ‘back-casting’ popu-

60 lation dynamics into historical environmental regimes; while rarely done (Smith
61 *et al.*, 2005), this approach may provide valuable insight regarding when and why
62 populations fell into extinction debt.

63 Many studies of climate-demography relationships focus on single climate vari-
64 ables that are known to be a dominant component of climate change and / or
65 known to have a strong influence on the focal species (e.g., Van de Pol *et al.* 2010;
66 Iler *et al.* 2019; Jenouvrier *et al.* 2009). However, for many species, it is not always
67 apparent *a priori* which dimensions of climate are most important, and this poses
68 challenges for predicting population responses to climate change. Previous studies
69 have shown that different components of climate change may have independent
70 effects on different aspects of demography or physiology (Buckley & Kingsolver,
71 2012; Frederiksen *et al.*, 2008; Van de Pol *et al.*, 2010; Lynch *et al.*, 2014). Fur-
72 thermore, different life stages (e.g., young vs old) and different vital rate processes
73 (e.g., growth, survival, reproduction) may differ in the magnitude and even di-
74 rection of their responses to single climate drivers (Doak & Morris, 2010; Dybala
75 *et al.*, 2013; Morrison & Hik, 2007; Tenhumberg *et al.*, 2018), and single life stages
76 or vital rates may be affected by multiple drivers (Dalglish *et al.*, 2011; Williams
77 *et al.*, 2015; Frederiksen *et al.*, 2008; Sletvold *et al.*, 2013). Ultimately, the influ-
78 ence of climate on population growth depends on the sensitivities of vital rates
79 to climate drivers and the sensitivities of λ to the vital rates, integrated across the
80 life cycle (McLean *et al.*, 2016; Ådahl *et al.*, 2006). These complications, common
81 to environmentally explicit demographic studies (Ehrlén *et al.*, 2016), highlight
82 the value of leveraging long-term data to gain resolution of climate drivers and the
83 importance of accounting for demographic complexity across the life cycle.

84 We used long-term demographic data to study climate-dependent population

85 dynamics of a long-lived Chihuahuan desert cactus persisting under extinction
86 debt. Our previous work with the tree cholla cactus (*Cylindriopuntia imbricata*
87 Haw. D.C.) (Cactaceae) indicated, with >95% certainty, that our focal population
88 in the northern Chihuahuan Desert (New Mexico, USA) is in decline (stochastic
89 population growth rate $\lambda_S < 1$) despite current densities that are reasonably high
90 (Ohm & Miller, 2014; Miller *et al.*, 2009; Elderd & Miller, 2016). This region has
91 experienced strong climatic fluctuations over the past century, including several
92 decadal-scale droughts interrupted by relatively wet periods (Peters *et al.*, 2015).

93 Our study was conducted in the following steps. First, we characterized climate
94 variation and change in our northern Chihuahuan desert study region over the past
95 century. Second, we estimated vital rate responses to inter-annual climate vari-
96 ation during the demographic study period (2004–2017). We hypothesized that
97 high-sensitivity vital rates (those that strongly influence λ) would be less respon-
98 sive environmental variability than low-sensitivity vital rates (Pfister, 1998). Third,
99 we back-casted climate-dependent demography to determine whether the past cen-
100 tury included periods that were favorable for population growth, thus testing the
101 hypothesis that recent climate change has driven this population into extinction
102 debt. Our analysis relied on a Bayesian framework that incorporates key sources
103 of uncertainty into our back-cast. Finally, we asked whether the components of
104 climate that are changing most strongly in this system are the same climate com-
105 ponents that most strongly influence cactus demography.

Materials and methods

Focal species, study site, and demographic data collection

Tree cholla cactus is widely distributed throughout desert and grassland habitats of the southwest U.S. and northern Mexico. These long-lived plants (40-plus years) grow through the production and elongation of cylindrical stem segments. These vegetative structures as well as flowerbuds are initiated in late spring. Flowering occurs in early summer and stem segment elongation takes place during the remainder of the growing season. For climate analyses, we divide the calendar year into warm-season months (May through September), when stem elongation, flowering, and seed production occur, and cool-season months (October through April).

This study was conducted at the Sevilleta National Wildlife Refuge (SNWR), a Long-Term Ecological Research site (SEV-LTER) in central New Mexico and near the center of this species' geographic distribution. Our study population occurs in the Los Piños mountains at an elevation of 1790 m. Tree cholla are a dominant component of the vegetation in this area (0.1 m^{-2} : Miller *et al.* 2009), along with oaks, yucca, Piñon pine, and the grasses *Bouteloua gracilis* and *B. eriopoda*.

The present study relies on long-term (2004–2017) demographic data on individual-level measures of growth, survival, and reproduction recorded from tagged plants in the Los Piños population that were censused in late May each year. This was a pre-breeding census that corresponds to the initiation of vegetative and reproductive structures (Fig. C1). We treat May 1 as the start of the transition year (coincident with the start of the warm-season months). There were a total of 1172 unique individuals in the data set and 7442 transition-year observations from 4–8

plots or spatial blocks depending on the year. Full details of the study design and data collection are given elsewhere (Miller *et al.*, 2009; Ohm & Miller, 2014; Elder & Miller, 2016).

Climate data

Our goal was to connect inter-annual variation in demography to corresponding variation in temperature and precipitation. SEV-LTER collects climate data from a network of meteorological stations throughout SNWR. While the SEV-LTER climate data cover years of our demographic data collection, our intention was to back-cast demographic performance farther back into the 20th century. We therefore gathered climate data from ClimateWNA v5.60 (Wang *et al.*, 2016), a software package that uses PRISM (Daly *et al.*, 2008) and WorldClim (Hijmans *et al.*, 2005) data to calculate downscaled data for western North America based on location and elevation, going as far back as 1900. We derived seasonal estimates (warm- and cool-season) of total precipitation and mean, minimum, and maximum temperature from monthly climate data, for a total of eight variables. Months were aligned to correspond to demographic transition years rather than calendar years, which means the cool-season climate for a transition year beginning in May of year t spans October of year t through April of year $t + 1$ (Fig. C1).

To reduce the dimensionality of the climate data, we conducted Principal Components Analysis (PCA) on the eight climate variables for the years 1900-2017, with climate values scaled to unit variance. We estimated the variance in the raw climate data explained by each PC and the variable loadings, which give the correlations between original variables and PC values. PCA allowed us to rank the

153 magnitudes of multiple aspects of climate variation and change by examining how
154 warm- and cool-season variables loaded onto the ranked PC axes.

155 By relying on downscaled, interpolated climate data instead of direct observa-
156 tions from meteorological stations we are trading off local resolution in favor of
157 more historical years of data. We quantified this loss of resolution by comparing
158 predictions from ClimateWNA to SEV-LTER data for years that they over-lapped,
159 using the SEV-LTER meteorological station that was nearest our study popula-
160 tion (Appendix A). We found that the two data sets were generally well correlated
161 (Table A1, Fig. A1,A2), which bolstered our confidence in ClimateWNA for back-
162 casting demographic responses to climate over the historical record. We further
163 explored the implications of using downscaled data by repeating all of our analy-
164 ses (described next) with SEV-LTER meteorological data and comparing results
165 between the two data sources (Appendix A).

166 Statistical estimation of climate-dependence

167 We fit generalized linear mixed effects models in a hierarchical Bayesian framework
168 to quantify climate dependence in demographic vital rates, as captured by three
169 principal components of climatic variability. The choice of three PCs was based
170 on results of parallel analysis (Fig. A3), a statistical method for determining how
171 many components to retain (Franklin *et al.*, 1995). There were four vital rates
172 measured in the long-term study for which we could estimate climate dependence:
173 survival from year t to year $t+1$, individual growth (change in size from year
174 t to year $t+1$), probability of flowering in year t , and the number of flowerbuds
175 produced year in t , given that a plant flowered. Survival and growth from year $t-1$

176 to t were dependent on size in year $t - 1$, and the climate covariate corresponded
 177 to the climate year $t - 1$ to t . Reproductive status and fertility in year t were
 178 dependent on size in year t and on climate from $t - 1$ to t . This timing of size
 179 and climate effects was intended to match processes in the population model (Fig.
 180 C1). We did not quantify climate-dependence in seedling recruitment. While we
 181 searched plots each year and added newly detected plants to the census, we could
 182 not confidently assign a birth year to these new additions (seedlings require several
 183 years of growth before they are consistently detectable in our census) so we do not
 184 know the climatic conditions under which they recruited.

185 All of the models for climate-dependent vital rates used the same linear predic-
 186 tor for the expected value (μ) but applied a different link function ($f(\mu)$) depending
 187 on the distribution of the observations:

$$\begin{aligned}
 f(\mu) = & \beta_0 + \beta_1 x + \\
 & \rho_1^1 PC1 + \rho_2^1 PC1^2 + \rho_3^1 x PC1 + \\
 & \rho_1^2 PC2 + \rho_2^2 PC2^2 + \rho_3^2 x PC2 + \\
 & \rho_1^3 PC3 + \rho_2^3 PC3^2 + \rho_3^3 x PC3 + \\
 & \phi + \tau
 \end{aligned} \tag{1}$$

188 The linear predictor includes a grand mean intercept (β_0) and size-dependent
 189 slope (β_1). The size variable x is the natural logarithm of plant volume ($\log_e(cm^3)$),
 190 which was standardized to mean zero and unit variance for analysis. Other fixed-
 191 effect coefficients (ρ) correspond to climate variables and climate \times size inter-
 192 actions. We include quadratic terms for climate to account for the possibility of

193 non-monotonic climate responses. Climate coefficient (ρ) superscripts correspond
194 to each PC, and subscripts correspond to linear, quadratic, and size-interaction ef-
195 fects. Finally, the linear predictor includes normally distributed random effects for
196 plot-to-plot variation ($\phi \sim N(0, \sigma_{plot})$) and year-to-year variation that is unrelated
197 to climate effects captured by PCs 1-3 ($\tau \sim N(0, \sigma_{year})$). The year random-effect
198 can be interpreted as inter-annual variability in demography that cannot be ex-
199 plained by the climate PCs. We used stochastic variable selection in a Bayesian
200 framework to reduce model complexity, dropping coefficients that were effectively
201 zero with $\geq 90\%$ certainty. Complete methods for variable selection are provided
202 in Appendix B.

203 The growth data were normally distributed; this model applied the identity
204 link and included an additional parameter for residual variance. We explored size-
205 dependence in the residual variance of growth (which determines how individuals
206 are distributed around their expected future size) but found that this led to poorer
207 model fits, so we proceeded to assume a constant value. The survival and flower-
208 ing data were Bernoulli distributed, and these models applied the logit link func-
209 tion. The fertility data (flowerbud counts) were modeled as Poisson-distributed,
210 including an individual-level random effect to account for overdispersion. All co-
211 efficients were given vague priors. We evaluated model fits using posterior predic-
212 tive checks (Elder & Miller, 2016). All models were fit using JAGS (Plummer
213 *et al.*, 2003) and R2JAGS (Su & Yajima, 2012). Analysis code is available at
214 https://github.com/texmiller/cholla_climate_IPM.

215 Demographic modeling

216 Model description

217 The statistical models described above formed the backbone of the integral projec-
218 tion model (IPM) that we used to estimate population growth in variable climate
219 environments. Following previous studies (Compagnoni *et al.*, 2016; Ohm & Miller,
220 2014; Elderd & Miller, 2016), we modeled the life cycle of *C. imbricata* using con-
221 tinuously size-structured plants, $n(x)$, and two discrete seed banks ($B_{1,t}$ and $B_{2,t}$)
222 corresponding to 1 and 2-year old seeds:

$$B_{1,t+1} = \kappa \delta \int_L^U P(x, \mathbf{c}_{t-1}; \alpha_t^P) F(x, \mathbf{c}_{t-1}; \alpha_t^F) n(x)_t dx \quad (2)$$

$$B_{2,t+1} = (1 - \gamma_1 B_{1,t}) \quad (3)$$

223 Functions P and F give the probability of flowering and the number of flowerbuds
224 produced, respectively, for an x -sized plant. The vector \mathbf{c}_{t-1} contains the climate
225 PC values for climate-year $t - 1$, which affects flowering and fertility in year t , and
226 hence the 1-year old seed bank in year $t + 1$. Parameters α_t^P and α_t^F are random
227 year effects estimated from the statistical models. The integral is multiplied by
228 the number of seeds per fruit (κ) and probability of seed dispersal/survival (δ) to
229 give the number of seeds that enter the 1-year old seed bank. Parameters L and U
230 are the lower and upper bounds, respectively, of the plant size distribution. Plants
231 can recruit out of the 1-year old seed bank with probability γ_1 or transition to the
232 2-year old seed bank with probability $(1 - \gamma_1)$. Seeds in the 2-year old seed bank
233 are assumed to either germinate (probability γ_2) or die.

234 Continuous-size dynamics were given by:

$$n(y)_{t+1} = (\gamma_1 B_{1,t} + \gamma_2 B_{2,t}) \eta(y) \omega + \int_L^U S(x, \mathbf{c}_t; \alpha_t^S) G(y, x, \mathbf{c}_t; \alpha_t^G) n(x)_t dx \quad (4)$$

235 The first term indicates recruitment from the seed banks to size y , where $\eta(y)$
 236 gives the seedling size distribution, assumed normal with mean μ_s and standard
 237 deviation σ_s . Mortality between germination (late summer) and the yearly demo-
 238 graphic census (May) is accounted for with survival probability ω . In the second
 239 term, functions S and G give the probabilities of surviving to year $t + 1$ and grow-
 240 ing to size y , respectively, for an x -sized plant in year t . Climate-dependence and
 241 random year effects are included as in Eq. 2, except the timing of climate effects
 242 is shifted such that growth and survival from t to $t + 1$ are affected by climate over
 243 the same interval (Fig. C1). As above, survival and growth functions also take
 244 time-varying random intercepts. Field data used to estimate seed and seed bank
 245 parameters are described elsewhere (Compagnoni *et al.*, 2016; Elderd & Miller,
 246 2016). All parameter estimates are provided in Table C1.

247 Model analysis

248 For analysis, we discretized x into b bins, replacing the continuous kernel with an
 249 b -by- b matrix (because our model also included two additional discrete states, the
 250 final projection matrix had dimensions $b + 2$ -by- $b + 2$). We used $b = 200$ bins. We
 251 extended integration limits L and U to avoid unintentional “eviction” (Williams
 252 *et al.*, 2012).

253 We estimated the asymptotic population growth rate λ as the dominant eigen-

254 value of the discretized IPM kernel. We compared the observed size distribution
 255 and the predicted distribution at the long-term mean climate ($PC_1 = PC_2 =$
 256 $PC_3 = 0$) and found generally good agreement (Fig. C2). We then evaluated how
 257 λ responded to climate variation by first varying each climate PC independently,
 258 holding the other two fixed at their long-term mean. Second, we back-casted λ
 259 over the entire climatological record that we had available (1900–2017), which gen-
 260 erated a time series of λ_t . We used linear regression to test for temporal trends
 261 in λ over this period. We incorporated two types of uncertainty into back-casted
 262 values of λ : imperfect knowledge of the parameter values (“estimation error”) and
 263 year-to-year fluctuations that were not related to climate (“process error”); the
 264 latter was estimated from the variances of random year effects. For the years of
 265 demographic data collection (2004–2017), we additionally quantified the deviations
 266 between predicted λ based solely on climate and “observed” λ that reflects climate
 267 and non-climate year effects (quotations indicate that these are the asymptotic pre-
 268 dictions given the vital rates observed in that year). We also conducted a similar
 269 analysis of λ_S using a 10-year sliding window (Appendix C), and we explored the
 270 consequences of extrapolating vital rate responses to climate values more extreme
 271 than those observed during the study period (Appendix D).

Finally, we used Life Table Response Experiments (LTREs) to decompose
 which combinations of climate PCs and vital rate responses were most strongly
 responsible for temporal fluctuations in the back-casted time series λ_t . We used
 a fixed-design LTRE (Caswell, 2001) where λ_t was defined as a linear function of

climate predictors:

$$\lambda_t = \bar{\lambda} + \sum_{i=1}^3 \nu_i PC_{i,t} \quad (5)$$

There is no error term because, in this analysis, climate PCs are assumed to be the sole drivers of fluctuations in λ_t . The coefficient for each climate PC was approximated as:

$$\nu_i \approx \sum_{j=1}^n \frac{\partial \bar{\lambda}}{\partial \theta_j} \frac{\partial \theta_j}{\partial PC_i} \quad (6)$$

272 The LTRE approximation is based on the product of the sensitivity of λ to the vital
 273 rates (θ), evaluated at the long-term mean climate ($PC_1 = PC_2 = PC_3 = 0$), and
 274 the sensitivity of the vital rates to climate, summed over all vital rates. Because
 275 LTRE components are additive, we summed LTRE estimates over the intercept
 276 and slope of each vital rate function so that we could interpret the results in terms
 277 of vital rate contributions.

278 Results

279 Climate trends

280 Three principal components cumulatively explained 73.3% of the inter-annual vari-
 281 ation in climate (Figure 1A). PC1 was dominated by inter-annual differences in
 282 temperature and precipitation, regardless of season, and the three components
 283 of temperature (mean, min, max) loaded similarly onto this component (Figure
 284 1B). Over the last century, PC1 trends have fluctuated, with prolonged stretches

285 of warm and dry years (the 1950s and early 2000s) and other periods of cool
286 and wet years (early 1900s and 1970s-80s), though the overall temporal trend for
287 PC1 was negative. The decline per-year was nearly five times stronger since 1970
288 compared to the long-term average (Fig. 1C), suggesting an accelerating trajec-
289 tory of warmer and drier years. PC2 was strongly driven by cool-season climate,
290 especially precipitation, such that greater values corresponded to wetter winters
291 with low temperature maxima and high temperature minima (Figure 1B). Warm-
292 season temperatures also loaded positively onto this axis to a lesser degree (Figure
293 1B). PC2 has increased since 1900 and the change per-year was nearly four times
294 stronger since 1970 (Figure 1D), indicating an accelerating trend of wetter cool
295 seasons with moderate winter temperatures. Lastly, PC3 was correlated with a
296 combination of warm- and cool-season climate variables. The strongest variable
297 loadings on this component were minimum and mean temperatures in the cool
298 season and warm-season precipitation. Temporal trends for PC3 showed weak de-
299 clines since 1900, corresponding to milder winters with higher minimum and mean
300 temperatures and wetter warm seasons; this trend has been slightly stronger since
301 1970 (Figure 1E).

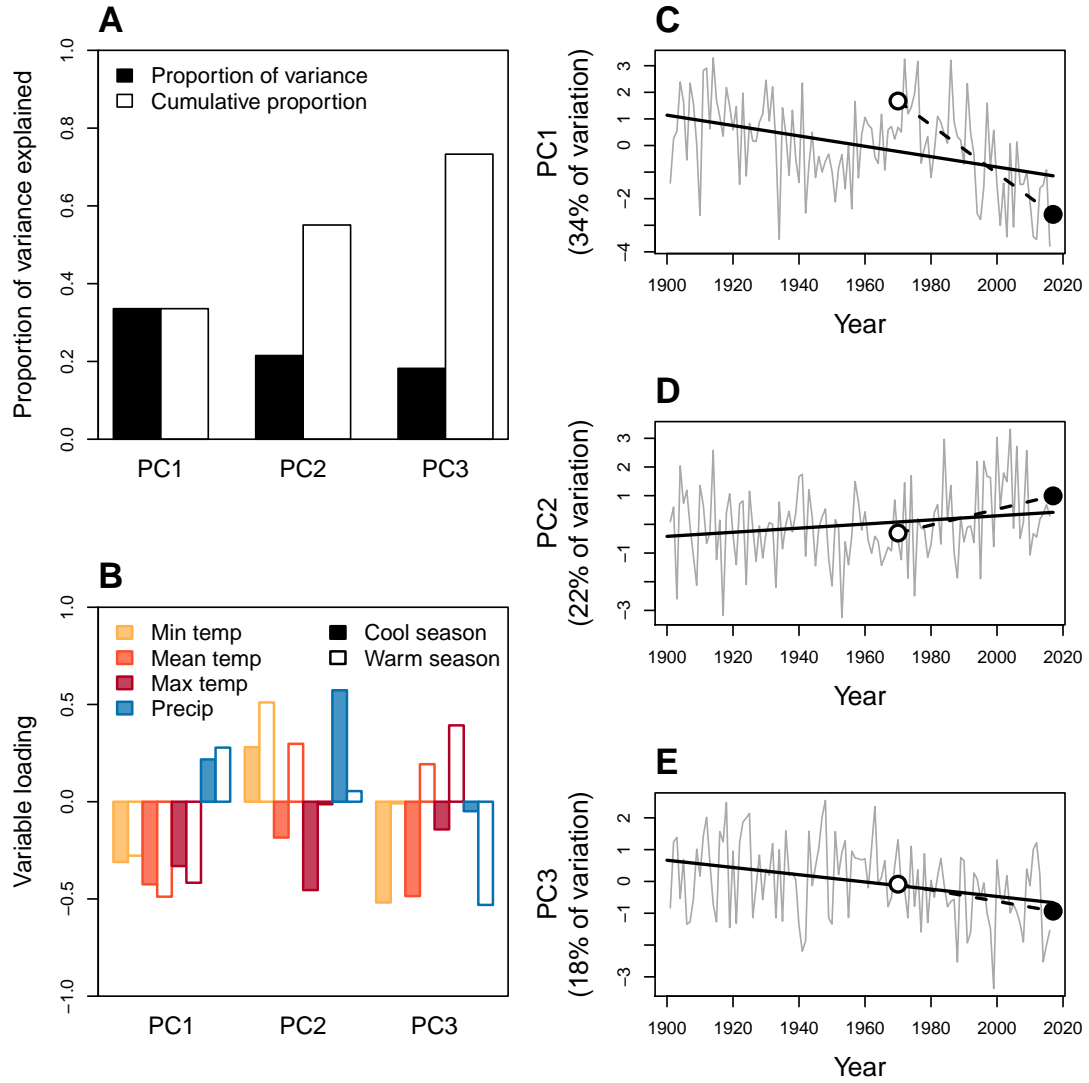


Figure 1: Principal components analysis (PCA) of inter-annual climate variability at SNWR, 1901–2017. **A**, Proportion and cumulative proportion of variation in seasonal temperatures (minimum, mean, maximum) and precipitation explained by the first three PCs. **B**, Loadings of seasonal climate variables onto PC1-3. Because climate data were standardized to mean zero and unit variance, loadings can be interpreted as the correlation between the climate variable and the PC. **C–E**, Time series of PC values, with regression lines showing long-term trends since 1901 (solid lines) or 1970 (dashed lines); open and filled points indicate the years 1970 and 2017, respectively, and correspond to the same shapes in Fig. 3

Vital rate responses to climate

Demographic vital rates estimated from long-term data (survival, growth, reproductive status, and fertility of flowering plants) were least responsive to PC1, the dominant axis of climate variability and change. All of the vital rates were strongly, positively size-dependent but there was heterogeneity in the magnitude and sign of responses to different dimensions of climate variability. Figure 2 shows vital rate data and fitted statistical models following variable selection procedures that eliminated coefficients that were weakly supported (Table B1). There was very little support for coefficients of quadratic climate effects (Table B1), indicating that responses to climate were monotonic over the range of variation we observed.

For PC1, there was a weak reduction in survival probability (especially for smaller plants; Fig. 2A) and a moderate reduction in flowering probability (especially for larger plants; Fig. 2G) at higher PC values, i.e., in cooler and wetter years. Fertility of flowering plants was not responsive to PC1 variation (Fig. 2J) and growth was not responsive to any of the climate PCs (Fig. 2D,E,F). There were positive responses to PC2 in survival (Fig. 2B), flowering probability (Fig. 2H), and fertility of flowering plants (Fig. 2K), indicating that these vital rates benefitted from years with wetter cool seasons. Responses to PC3 varied in sign, with survival increasing with decreasing PC values (years with mild winter temperature minima and wet summers) and reproductive rates increasing with increasing PC values (years with low winter minima and dry summers) (Fig. 2C,I,L).

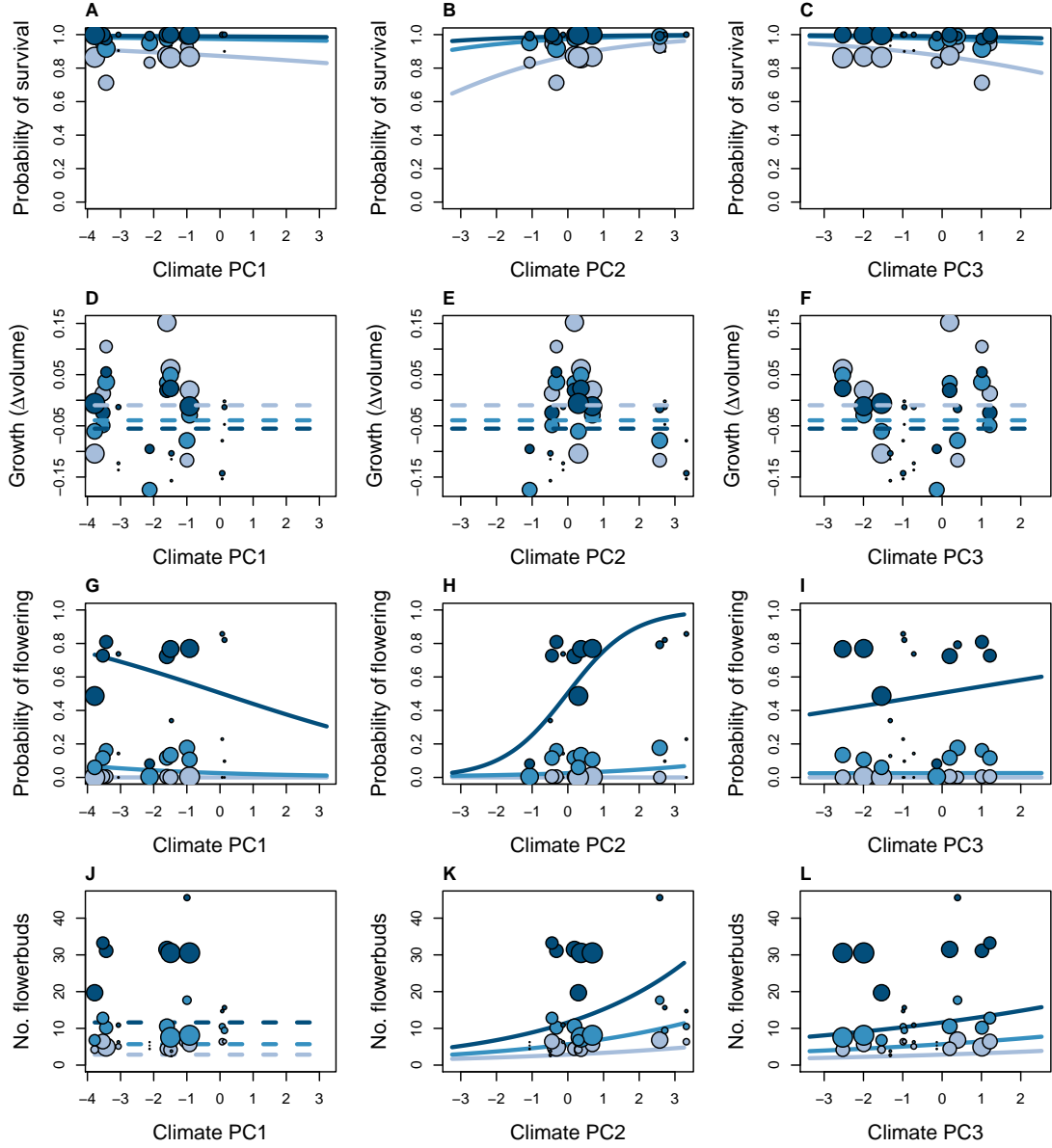


Figure 2: Climate- and size-dependent variation in survival (A-C), growth (D-F), flowering (G-I), and fertility of flowering plants (J-L) in relation to three principal components of seasonal climate variation (columns). For visualization only, the plant size distribution was discretized into three groups (small, medium, and large, corresponding to increasingly dark shading). Points show means for each size group in each year, where different years have unique PC values and point size is proportional to sample size for each size group in each year. Lines show fitted statistical models using posterior mean parameter values, with shading corresponding to size groups. Dashed lines indicate that the climate predictor was not statistically supported. Ranges of x -axes show the climate extrapolation that was required for back-casting.

Climate-dependent population growth

The population growth rate λ was predicted to increase with decreasing values of PC1 (hotter, drier years), holding other PCs fixed at their long-term average (Fig. 3A). Population growth was also predicted to increase with increasing values of PC2 (wetter cool seasons; Fig. 3B). Population growth was more sensitive to PC2 than PC1, such that the predicted change in λ from 1970 to 2017 was slightly greater for PC2 even though PC1 exhibited much greater change than PC2 over this period. Finally, greater values of PC3 (colder winters and drier summers) were predicted to cause declines in population growth, indicating that negative effects on cactus survival outweighed positive effects of PC3 on reproduction (Fig. 2). PC3 has changed relatively little since 1970 but this was associated with a change in λ of about half the magnitude to the response to relatively large change in PC1. Overall, recent climate change in each of the principal components, in isolation, has been in the direction that favors increased population growth (Fig. 1, 3). However, mean estimates for population growth rates were consistently below replacement level for all climate PC values, and the posterior probability densities rarely met or exceeded $\lambda = 1$.

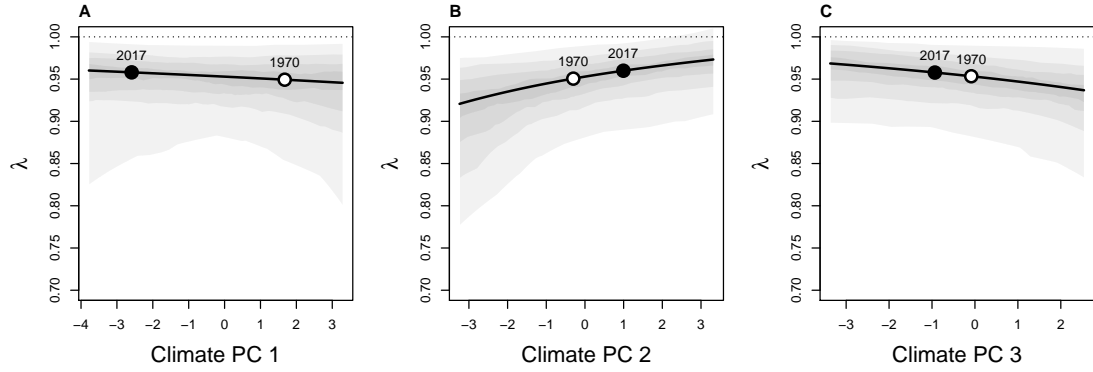


Figure 3: Predicted asymptotic population growth rate (λ) in response to three principal components of inter-annual climatic variation (A-C). For each panel, the indicated principal component is varying while the others are held at zero (the average value). Lines show the expected relationships based on posterior mean parameter values and shaded contours show the 25,50,75, and 95% credible intervals, representing uncertainty in demographic parameters. Points highlight the change the PC value (on the x -axis) between 1970 and 2017, based on the regression lines shown in Fig. 1, and the predicted corresponding change in λ (y -axis).

Back-casting population growth

Figure 4A shows the back-casted time series of λ accounting for inter-annual variation in all three PC components. For the observation years (2004-2017), the three climate PCs explained 60% of the inter-annual variation in λ (points in Fig. 4A). Thus, even with relatively strong climate-demography associations (Fig. 2), there was substantial uncertainty in our back-casted estimates of λ . The shaded region in Fig. 4A represents the combined uncertainty arising from heterogeneity in vital rates across years that could not be attributed to the climate PCs (process error) and imperfect knowledge of the underlying parameters (estimation error). In Appendix Fig. C3, we show that process error contributed the majority of the

350 total uncertainty.

351 Despite uncertainty in our back-cast, the results indicated that λ has likely
352 remained below replacement levels for more than a century; there was no evidence
353 that climate change drove this population into extinction debt. To the contrary,
354 there was a positive temporal trend ($\frac{\Delta\lambda}{\Delta Year} > 0$), suggesting a trajectory of increas-
355 ing population growth rates through time (Fig. 4B). There was wide uncertainty
356 in the rate of change but the posterior probability distribution indicated that it
357 was 2.5 times more likely that λ has increased than decreased. Furthermore, the
358 median rate of increase was 2.27 times greater since 1970 compared to the overall
359 trend since 1900 (Fig. 4B), corresponding to the acceleration of climate change
360 (Fig. 1). There was greater uncertainty in $\frac{\Delta\lambda}{\Delta Year}$ since 1970 because this estimate
361 was based on fewer years. Under the trajectory since 1970, population growth
362 was expected to reach the viability threshold ($\lambda = 1$) in the year 2057 (Fig. 4C);
363 accelerating climate change would advance this transition to viable growth rates.

364 In Appendix D, we show that our inference that λ is likely increasing in response
365 to climate change holds even with a more conservative approach that does not
366 extrapolate vital rate responses beyond the climate extremes of the observation
367 years. Furthermore, in Appendix A, we show that year-specific estimates of λ
368 were correlated between models built with downscaled climate data versus on-site
369 meteorological measurements, for years in which they over-lapped (Fig. A8, Fig.
370 A7). This suggests that our qualitative inference regarding the positive temporal
371 trend in λ is robust to the loss of resolution associated with downscaled climate
372 data.

373 The stochastic population growth rate (λ_S) showed a similar trend of $\lambda_S < 1$
374 and increasing population growth rates over the past 120 years (Fig. C4). The

375 stochastic growth rate reveals the effects of multi-year climate events, such as the
 376 runs of good years in the 1940s and 2000s.

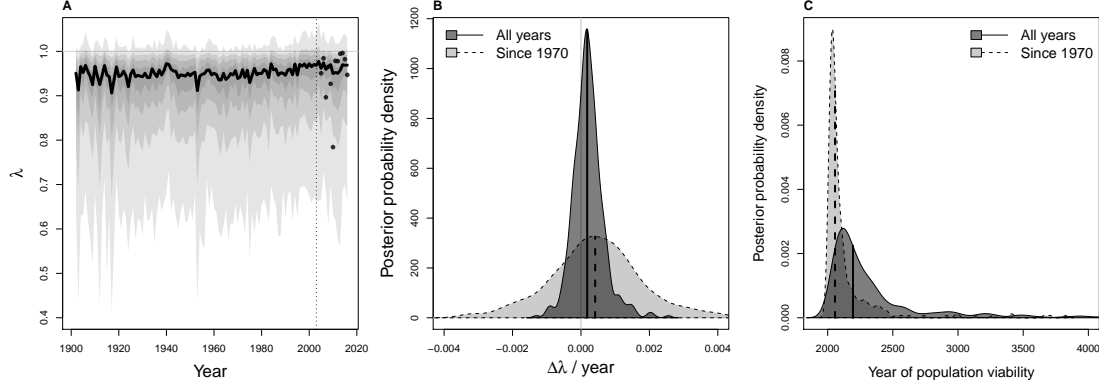


Figure 4: **A**, Posterior probability distribution for the time series of asymptotic population growth rates (λ) predicted based on inter-annual variation in three climate PCs. Thick black line shows the mean prediction and shaded regions show the 25, 50, 75, and 95% credible regions accounting for both parameter uncertainty and process error (year-to-year variation in vital rates that was unrelated to climate). Dashed vertical line separates years that were back-casted versus years that were directly observed. The observation years (2004 and later) include estimates for year-specific population growth rates (points), captured statistically as year-specific random effects in the vital rates. **B**, Posterior distributions for the rate of temporal change in population growth ($\frac{\Delta\lambda}{\Delta Y_{\text{ear}}}$). Dark grey shows the rate of change across all years shown in **A** and light grey shows the rate of change since 1970. Vertical lines show median values. **C**, Posterior distributions for the year of population viability ($\lambda = 1$) for the subset of posterior samples for which $\frac{\Delta\lambda}{\Delta Y_{\text{ear}}} > 0$. Shading and lines as in **B**.

377 Life Table Response Experiment

378 Life Table Response Experiments (LTRE) provided a decomposition of how λ
 379 responded to long-term climate trends (1900-2017), allowing us to understand the
 380 relative importance of different dimensions of climate variability and vital rate
 381 responses to them. LTRE results indicated that survival responses to climate

were the overwhelming driver of temporal trends in λ (Fig. 5). Individual growth made no contribution to these trends because it was unresponsive to climate (Fig. D,E,F), whereas flowering and fertility were responsive to climate but their role was relatively small and imperceptible in Fig. 5. Furthermore, survival responses to climate PC2 were the dominant driver of temporal trends, followed by PC3 and then PC1. Collectively, responses to PC2 and PC3 accounted for 91% of the overall climate effect in back-casted values of λ .

Discussion

Understanding and predicting the effects of environmental change on plant demography and population dynamics are urgent challenges. The integration of long-term data with environmentally explicit demographic models provides a powerful vehicle for meeting these challenges and may aid in identifying processes that drive some populations into decline. By reconstructing 117 years of climate-dependent demography, we tested the hypothesis that the extinction debt of our study population was a consequence of recent climate change. Our results [fail to support this hypothesis and](#) suggest the opposite: *C. imbricata* is likely a climate change “winner”, on an accelerating trajectory toward replacement-level population growth within 37 years if current climate change trends persist, and sooner if they accelerate. We further show that the strongest feature of climate change in this system was not the main driver of population responses. Instead, temporal trends in population viability were dominated by more subtle climatic factors with relatively weak signals of recent change. Below, we interpret these results in greater detail and discuss their broader significance.

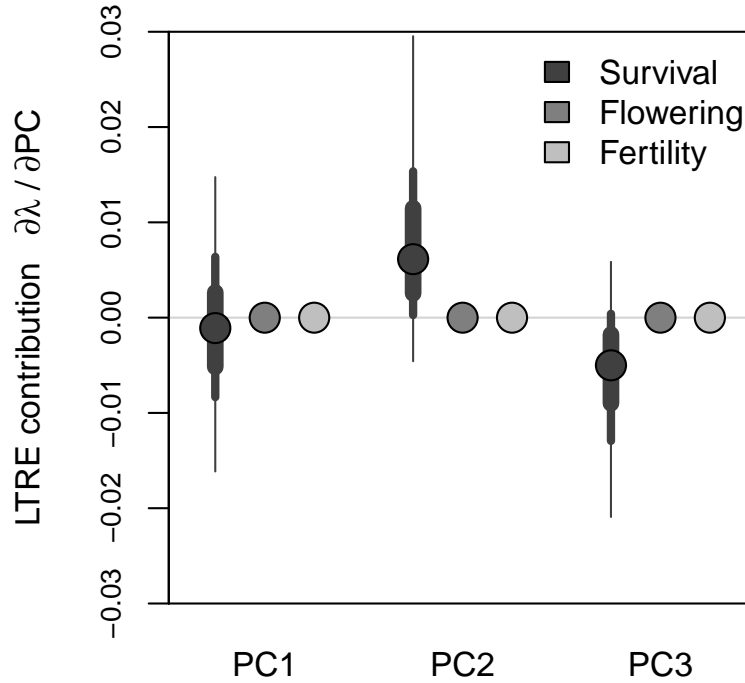


Figure 5: LTR decomposition of climate-driven inter-annual variability in population growth rates. Lines of decreasing thickness show the 50, 75 and 95 percentiles of the posterior distributions of the vital rate parameters, and points show the median. Shading corresponds to different vital rates (survival, flowering, and fertility) Posterior distributions for flowering and fertility are imperceptible on this scale.

405 Until recently, few plant demographic studies explicitly considered climatic
 406 drivers of inter-annual variation (Ehrlén *et al.*, 2016; Crone *et al.*, 2011), though
 407 this is rapidly changing. We are aware of no previous studies that have compared
 408 the magnitudes of different aspects of climate change alongside the magnitudes of

409 demographic responses to those changes. However, we suspect that our key finding
410 – that the strongest dimension of climate change was not the strongest driver of
411 demography – may be common, since at the heart of this result lies the difference
412 between annual climate trends (captured by PC1) versus seasonal trends (PCs 2
413 and 3). Annual rainfall totals in our region have been decreasing but more of the
414 annual rainfall has been falling in the cool season, consistent with previous climata-
415 logical studies that suggest a shift from warm- to cool-season precipitation (Cook &
416 Seager, 2013; Cook *et al.*, 2015; Petrie *et al.*, 2014). Similarly, annual temperatures
417 have been increasing in our study region but it was cool-season warming, specif-
418 ically, that was most important for *C. imbricata* demography. Many plant and
419 animal life histories operate on seasonal schedules and may therefore be more sen-
420 sitive to seasonal redistribution of rainfall and temperature than to climate effects
421 that manifest over an entire year. Our results are consistent with previous studies
422 that demonstrate the importance of considering seasonal, not annual, drivers of
423 plant demographic responses (Selwood *et al.*, 2015; Williams *et al.*, 2015; Dahlgren
424 *et al.*, 2016). Some recent studies have taken a finer-grained approach, connecting
425 plant responses to weather events on monthly, weekly, or even daily time scales
426 (Teller *et al.*, 2016; Tenhumberg *et al.*, 2018; Shriver, 2016). For tractability, we
427 did not explore lagged climate effects beyond one year, though methods for doing
428 so are rapidly developing (Teller *et al.*, 2016; Tenhumberg *et al.*, 2018; Ogle *et al.*,
429 2015). Finding the appropriate timing and resolution of climate covariates is an
430 important area for future work in this system and more generally.

431 Rigorously accounting for various types of uncertainty is another an important
432 area in the development of environmentally explicit models for forecasting or back-
433 casting. Even with strong climate-demography relationships detected with our

434 unusually long-term data set, climate drivers accounted for less than two-thirds of
435 the inter-annual variation in λ during the study years. It was therefore important
436 to place our predictions for historical growth rates in the context of the substantial
437 uncertainty that arose from process error: all the additional, unspecified ways
438 that years may differ. We have emphasized the positive trajectory of population
439 viability as the most likely trend in λ , but this should be interpreted in light
440 of the probability distributions that we provide (Fig. 4) – that is, with nuance
441 and appropriate caution¹. As ecologists are increasingly called upon to forecast
442 responses to change in climate drivers, it will be essential to do so in a probabilistic
443 framework that accommodates process error, i.e., the variability *not* explained by
444 climate drivers. Defining the temporal or spatial auto-correlation structure of
445 process error (which we did not attempt) may further improve forecasts or back-
446 casts.

447 Different aspects of a species' life cycle may respond in diverse ways to environ-
448 mental drivers (Doak & Morris, 2010; Villellas *et al.*, 2015), highlighting the addi-
449 tional importance of considering multiple vital rates for understanding responses
450 to global change. Our work was able to pinpoint which responses throughout the
451 life cycle were most important for the overall population response to climate. Our
452 results are consistent with previous findings that high-sensitivity vital rates (those
453 that strongly influence λ , in this case survival and growth) are buffered against en-
454 vironmental variability while low-sensitivity vital rates (flowering and fertility) may
455 exhibit wide fluctuations (Pfister, 1998). However, incomplete buffering of survival
456 led to greater mortality in years with cold and dry cool-seasons – years that are be-

¹By coincidence, the probability that λ is increasing (0.714) matched the probability of a Clinton victory in the 2016 U.S. presidential election: <https://projects.fivethirtyeight.com/2016-election-forecast/>

457 coming less frequent under climate change (Fig. 1) – and these survival responses
458 dominated the overall increase in population viability over the past 120 years
459 (Fig. 5). These results mirror a recent study of another long-lived perennial plant,
460 the alpine sunflower *Helianthella quinquinervis*, where reproductive responses to
461 climate drivers were strong but ultimately overwhelmed by weaker responses in
462 survival that more strongly affected population growth (Iler *et al.*, 2019). It is
463 commonly observed that demographic transitions related to growth and survival
464 are the most important determinants of population viability in species with long-
465 lived perennial life histories (Franco & Silvertown, 2004). It may therefore be a
466 general result that climate effects on growth and survival will be more consequen-
467 tial in long-lived perennials than effects on reproductive processes, even as the
468 latter exhibit greater sensitivity to climate, since perennials have many reproduc-
469 tive opportunities over potentially long lifespans (Dalglish *et al.*, 2010; Morris
470 *et al.*, 2008).

471 Our historical reconstruction of climate-dependent population growth indicated
472 that the climate has likely never been better for *C. imbricata* than it is now. This
473 result begs the question of how these plants have reached their current, relatively
474 high abundance, given over a century of population growth rates that were inferred
475 to fall well below replacement levels. Land use history – which is not incorporated
476 into our back-casted estimates – may have played a role. The Sevilleta NWR
477 was exposed to grazing for much of the 20th century until 1973. Previous work
478 suggests that cacti, and *C. imbricata* in particular, can increase in abundance
479 in response to grazing, due to livestock dispersing detached stem segment and
480 thus promoting asexual regeneration (Allen *et al.*, 1991). During our study, we
481 observed recruitment to be almost exclusively from seed (sexual and asexual re-

482 cruits are easily distinguishable), though it is possible that regeneration dynamics
 483 were different under historical grazing regimes. Grazing may have also promoted
 484 cactus populations through release of competitive interactions with grasses (Yu
 485 *et al.*, 2019). Thus, one hypothesis is that *C. imbricata* achieved current densities
 486 under the historical land use regime, and cannot maintain these densities in the
 487 absence of cattle grazing. For long-lived plants, it may take decades to centuries
 488 for full payment of extinction debt driven by land use changes (Lehtilä *et al.*,
 489 2016; González-Varo *et al.*, 2015). An alternative hypothesis is that, independent
 490 of grazing or other land use history, our study population may be located in sink
 491 habitat and maintained by dispersal from nearby populations that are more viable.
 492 Indeed, previous work showed that *C. imbricata* at lower (by ca. 100 m) elevations
 493 had positive population growth rates (Miller *et al.*, 2009) and may therefore act
 494 as source populations. Regardless of which process or processes best account for
 495 the persistence of a population that is currently inviable, our results indicate that
 496 it will more likely than not be ‘rescued’ by ongoing climate change. One caveat
 497 to this conclusion is that, beyond the mean climate trends we have described, fu-
 498 ture climate (and especially monsoon precipitation) in our region is expected to
 499 be more variable (Rudgers *et al.*, 2018; Cook *et al.*, 2015) and this may dampen
 500 population growth independently of mean conditions (Boyce *et al.*, 2006). How-
 501 ever, our stochastic demographic analysis, which accounts for increasing climate
 502 variability during the 20th century, also showed a positive trajectory of λ_S (Fig.
 503 C4).

504 Previous studies of cacti have emphasized their sensitivity to freezing as a con-
 505 straint on physiological performance and geographic distribution (Flores & Yeaton,
 506 2003; Kinraide, 1978; Nobel, 1984). In our study, we detected an important role

507 for winter minimum temperature and observed high mortality following record low
 508 winter temperatures over a multi-day deep-freeze in 2011 (this is the low outlier
 509 in Fig. 4A). As these freezing events become less frequent under climate change,
 510 we expect an increase in regional abundance and perhaps northern expansion of
 511 *C. imbricata*'s range, which currently extends to southern Colorado and is likely
 512 limited by winter minimum temperatures. This may be an issue of applied concern
 513 in the region since *C. imbricata* is considered undesirable **due to its unpalatabil-**
 514 **ity to livestock** (Allen *et al.*, 1991). The role of cool-season precipitation that we
 515 detected was more surprising. A majority of annual precipitation in the South-
 516 west US comes from warm-season monsoon events (Adams & Comrie, 1997) and
 517 these events play a critical role in vegetation dynamics (Notaro & Gutzler, 2012;
 518 Petrie *et al.*, 2014), especially for plants with C4 and CAM photosynthesis that
 519 are physiologically most active during the warm summer months. Previous cactus
 520 demographic studies have emphasized the role of summer monsoon precipitation
 521 (Winkler *et al.*, 2018; Bowers, 2005). Our results suggest that, despite its summer-
 522 adapted CAM photosynthetic pathway, *C. imbricata* is able to capitalize on cool-
 523 season moisture, and this was an important component of the positive demographic
 524 effects of recent climate change. Similarly, Salguero-Gomez *et al.* (2012) identified
 525 *Cryptantha flava* as **a species likely to benefit from climate change** due in part to
 526 seasonal redistribution of rainfall that will lengthen its growing season.

527 Our work highlights several considerations that may be relevant for studies of
 528 demographic back-casting in other systems. First, we faced a trade-off between
 529 temporal depth and local resolution of climate data. While downscaled climate
 530 interpolation (from ClimateWNA) and on-site measurements (from SEV-LTER)
 531 were correlated, they were not perfectly so (Appendix A); this was especially true

for temperature minima and maxima (Table A1), where downscaled data likely mis-estimate localized extremes. We prioritized the greater temporal coverage provided by downscaled data, which led an 18% reduction in how well climate explained inter-annual variation in λ , relative to on-site climate data (Appendix A). Consequently, reliance on downscaled data inflated the contribution of process error to our back-casted estimates (Appendix D), and made λ appear less responsive to climate than it likely was. It is particularly noteworthy that the downscaled climate data poorly captured the deep-freeze of winter 2011 (Fig. A1A). Poor demographic performance in this year was consequently attributed to a statistical random effect (Fig. 4A), though this was almost certainly a true climate effect. As expected, the on-site data predicted a lower λ value in this year than the downscaled data (Fig. A8). When available, climate data sources that break the trade-off between temporal depth and local resolution would provide the strongest foundation for accurate back-casting. When such resources are not available, quantifying the loss of resolution, as we have done (Appendix A), may be valuable for interpreting results.

Second, just like forecasting, demographic back-casting may require projection into climatic conditions that were represented poorly or not at all during the data collection period. This requires the assumption that the relationship between vital rates and climate covariates does not change or break down under conditions more extreme than observed. We found similar results whether or not we extrapolated demographic performance into unobserved conditions (Appendix D). This was a lucky break, reflecting the fact that the climate covariate requiring the most extrapolation (PC1) had the weakest effect on λ . In other cases, where important covariates must be extrapolated to no-analogue conditions, comparing results with

557 and without extrapolation (Appendix D) may be valuable for setting liberal and
558 conservative bounds on model projections. This approach may also aid in identi-
559 fying situations where experimental climate manipulations could help bridge the
560 gap between current and historic (or future) conditions.

561 Some additional limitations of our study warrant consideration in the inter-
562 pretation of our results. First, our treatment of climate dependence was limited
563 to four vital rate processes of established plants. Because we could not reliably
564 assign a birth year to new recruits, we did not incorporate climate dependence in
565 seedling recruitment. Previous studies of cactus demography suggest that seedling
566 recruitment may be highly sensitive to climate, especially monsoon precipitation
567 (e.g., Bowers 2005; Winkler *et al.* 2018). We suspect this is the case for *C. imbrici-*
568 *cata*, since germination usually coincides with late-summer rains (*T.E.X. Miller,*
569 *unpubl. data*). Because we did not model this process as climate-dependent, our
570 results for climate effects on population growth are conservative. However, con-
571 sistent with expectations for long-lived perennials, we know seedling recruitment
572 to have very low eigenvalue sensitivities (Elder & Miller, 2016), which suggests
573 that even large climate effects on this process may not strongly register in terms of
574 population growth. On the other hand, pulsed recruitment events perturb the size
575 distribution in ways that can importantly affect short-term (transient) dynamics
576 (Williams *et al.*, 2011), and may therefore warrant further study in this and other
577 pulsed-recruitment system.

578 To conclude, this study illustrates how long-term patterns of population growth
579 can be reconstructed (with potentially substantial but quantifiable uncertainty)
580 through climate-demography relationships observed on relatively short time scales.
581 This allowed us to evaluate the hypothesis that recent climate change has driven

582 *C. imbricata* in our region into extinction debt, a hypothesis that our data do
583 not support. Instead, this species is most likely benefitting from climate change,
584 largely due to its positive responses, especially in survival, to recent and ongoing
585 shifts in cool-season temperature and precipitation. Changes in cool-season climate
586 were not the strongest features of climate change, but they were nonetheless the
587 most important determinants of population responses. The more general lesson
588 for global change biologists is that relatively subtle dimensions of climate change
589 may trigger strong ecological responses.

590 Acknowledgements

591 This study was supported by the Sevilleta LTER (NSF LTER awards 1440478,
592 1655499, and 1748133) and by NSF Division of Environmental Biology awards
593 1543651 and 1754468. We thank the Sevilleta National Wildlife Refuge staff (es-
594 pecially J. Erz) for facilitating research access. We thank M. Evans and E. Schultz
595 for helpful discussions on modeling climate-demography relationships. Finally, we
596 thank the many students and colleagues have contributed to this long-term study,
597 especially M. Donald, A. Compagnoni, and B. Ochocki. Two reviewers provided
598 helpful feedback on our work.

599 Author contributions

600 TEXM initiated and maintains the long-term study. KC collected and analyzed
601 data and prepared a manuscript draft. TEXM finalized text and analyses. Both
602 coauthors approve this submission.

Data accessibility

All of the code for our statistical and demographic modeling is available at https://github.com/texmiller/cholla_climate_IPM and raw data will be published in parallel with this manuscript.

References

- Ådahl E, Lundberg P, Jonzen N (2006) From climate change to population change: the need to consider annual life cycles. *Global Change Biology*, **12**, 1627–1633.
- Adams DK, Comrie AC (1997) The north american monsoon. *Bulletin of the American Meteorological Society*, **78**, 2197–2214.
- Adler PB, Byrne KM, Leiker J (2013) Can the past predict the future? experimental tests of historically based population models. *Global change biology*, **19**, 1793–1803.
- Allen L, Allen E, Kunst C, Sosebee R (1991) A diffusion model for dispersal of *opuntia imbricata* (cholla) on rangeland. *The Journal of Ecology*, pp. 1123–1135.
- Bowers JE (2005) Influence of climatic variability on local population dynamics of a sonoran desert *platyopuntia*. *Journal of Arid Environments*, **61**, 193–210.
- Boyce MS, Haridas CV, Lee CT, Group NSDW, *et al.* (2006) Demography in an increasingly variable world. *Trends in Ecology & Evolution*, **21**, 141–148.
- Buckley LB, Kingsolver JG (2012) The demographic impacts of shifts in climate means and extremes on alpine butterflies. *Functional Ecology*, **26**, 969–977.

- 623 Caswell H (2001) *Matrix Population Models*. Sinauer Associates, Inc., Sunderland,
624 MA, 2 edn.
- 625 Compagnoni A, Bibian AJ, Ochocki BM, *et al.* (2016) The effect of demographic
626 correlations on the stochastic population dynamics of perennial plants. *Ecolog-
627 ical Monographs*, **86**, 480–494.
- 628 Cook B, Seager R (2013) The response of the north american monsoon to increased
629 greenhouse gas forcing. *Journal of Geophysical Research: Atmospheres*, **118**,
630 1690–1699.
- 631 Cook BI, Ault TR, Smerdon JE (2015) Unprecedented 21st century drought risk
632 in the american southwest and central plains. *Science Advances*, **1**, e1400082.
- 633 Crone EE, Menges ES, Ellis MM, *et al.* (2011) How do plant ecologists use matrix
634 population models? *Ecology letters*, **14**, 1–8.
- 635 Dahlgren JP, Bengtsson K, Ehrlén J (2016) The demography of climate-driven and
636 density-regulated population dynamics in a perennial plant. *Ecology*.
- 637 Dalglish HJ, Koons DN, Adler PB (2010) Can life-history traits predict the re-
638 sponse of forb populations to changes in climate variability? *Journal of Ecology*,
639 **98**, 209–217.
- 640 Dalglish HJ, Koons DN, Hooten MB, Moffet CA, Adler PB (2011) Climate influ-
641 ences the demography of three dominant sagebrush steppe plants. *Ecology*, **92**,
642 75–85.
- 643 Daly C, Halbleib M, Smith JI, *et al.* (2008) Physiographically sensitive mapping
644 of climatological temperature and precipitation across the conterminous united

645 states. *International Journal of Climatology: a Journal of the Royal Meteorological Society*, **28**, 2031–2064.

646

647 Dinno A (2018) *paran: Horn's Test of Principal Components/Factors*. URL <https://CRAN.R-project.org/package=paran>. R package version 1.5.2.

648

649 Doak DF, Morris WF (2010) Demographic compensation and tipping points in

650 climate-induced range shifts. *Nature*, **467**, 959.

651 Dullinger S, Gatttringer A, Thuiller W, *et al.* (2012) Extinction debt of high-

652 mountain plants under twenty-first-century climate change. *Nature Climate Change*, **2**, 619.

653

654 Dybala KE, Eadie JM, Gardali T, Seavy NE, Herzog MP (2013) Projecting de-

655 mographic responses to climate change: adult and juvenile survival respond

656 differently to direct and indirect effects of weather in a passerine population.

657 *Global Change Biology*, **19**, 2688–2697.

658 Ehrlén J, Morris WF (2015) Predicting changes in the distribution and abundance

659 of species under environmental change. *Ecology Letters*, **18**, 303–314.

660 Ehrlén J, Morris WF, von Euler T, Dahlgren JP (2016) Advancing environmentally

661 explicit structured population models of plants. *Journal of Ecology*, **104**, 292–

662 305.

663 Elderd BD, Miller TE (2016) Quantifying demographic uncertainty: Bayesian

664 methods for integral projection models. *Ecological Monographs*, **86**, 125–144.

665 Flores JL, Yeaton R (2003) The replacement of arborescent cactus species along a

666 climatic gradient in the southern chihuahuan desert: competitive hierarchies and
667 response to freezing temperatures. *Journal of arid environments*, **55**, 583–594.

668 Franco M, Silvertown J (2004) A comparative demography of plants based upon
669 elasticities of vital rates. *Ecology*, **85**, 531–538.

670 Franklin SB, Gibson DJ, Robertson PA, Pohlmann JT, Fralish JS (1995) Parallel
671 analysis: a method for determining significant principal components. *Journal of*
672 *Vegetation Science*, **6**, 99–106.

673 Frederiksen M, Daunt F, Harris MP, Wanless S (2008) The demographic impact
674 of extreme events: stochastic weather drives survival and population dynamics
675 in a long-lived seabird. *Journal of Animal Ecology*, **77**, 1020–1029.

676 George EI, McCulloch RE (1993) Variable selection via gibbs sampling. *Journal*
677 *of the American Statistical Association*, **88**, 881–889.

678 González-Varo JP, Albaladejo RG, Aizen MA, Arroyo J, Aparicio A (2015) Ex-
679 tinction debt of a common shrub in a fragmented landscape. *Journal of Applied*
680 *Ecology*, **52**, 580–589.

681 Hastings A, Abbott KC, Cuddington K, *et al.* (2018) Transient phenomena in
682 ecology. *Science*, **361**, eaat6412.

683 Hijmans RJ, Cameron SE, Parra JL, Jones PG, Jarvis A (2005) Very high reso-
684 lution interpolated climate surfaces for global land areas. *International Journal*
685 *of Climatology: A Journal of the Royal Meteorological Society*, **25**, 1965–1978.

686 Hooten MB, Hobbs N (2015) A guide to bayesian model selection for ecologists.
687 *Ecological Monographs*, **85**, 3–28.

- Hylander K, Ehrlén J (2013) The mechanisms causing extinction debts. *Trends in ecology & evolution*, **28**, 341–346.
- Iler AM, Compagnoni A, Inouye DW, Williams JL, CaraDonna PJ, Anderson A, Miller TE (2019) Reproductive losses due to climate change-induced earlier flowering are not the primary threat to plant population viability in a perennial herb. *Journal of Ecology*, **107**, 1931–1943.
- Jenouvrier S, Caswell H, Barbraud C, Holland M, Stroeve J, Weimerskirch H (2009) Demographic models and ipcc climate projections predict the decline of an emperor penguin population. *Proceedings of the National Academy of Sciences*, **106**, 1844–1847.
- Jenouvrier S, Holland M, Stroeve J, Serreze M, Barbraud C, Weimerskirch H, Caswell H (2014) Projected continent-wide declines of the emperor penguin under climate change. *Nature Climate Change*, **4**, 715.
- Kinraide TB (1978) The ecological distribution of cholla cactus (*opuntia imbricata* (haw.) dc.) in el paso county, colorado. *The Southwestern Naturalist*, pp. 117–133.
- Kuussaari M, Bommarco R, Heikkinen RK, *et al.* (2009) Extinction debt: a challenge for biodiversity conservation. *Trends in ecology & evolution*, **24**, 564–571.
- Lehtilä K, Dahlgren JP, Garcia MB, Leimu R, Syrjänen K, Ehrlén J (2016) Forest succession and population viability of grassland plants: long repayment of extinction debt in *primula veris*. *Oecologia*, **181**, 125–135.
- Lynch HJ, Rhainds M, Calabrese JM, Cantrell S, Cosner C, Fagan WF (2014) How

710 climate extremes—not means—define a species’ geographic range boundary via
711 a demographic tipping point. *Ecological Monographs*, **84**, 131–149.

712 Maschinski J, Baggs JE, QUINTANA-ASCENCIO PF, Menges ES (2006) Using
713 population viability analysis to predict the effects of climate change on the ex-
714 tinction risk of an endangered limestone endemic shrub, arizona cliffrose. *Con-*
715 *servation Biology*, **20**, 218–228.

716 McLean N, Lawson CR, Leech DI, van de Pol M (2016) Predicting when climate-
717 driven phenotypic change affects population dynamics. *Ecology Letters*, **19**,
718 595–608.

719 Miller TE, Louda SM, Rose KA, Eckberg JO (2009) Impacts of insect herbivory on
720 cactus population dynamics: experimental demography across an environmental
721 gradient. *Ecological Monographs*, **79**, 155–172.

722 Morris WF, Pfister CA, Tuljapurkar S, *et al.* (2008) Longevity can buffer plant and
723 animal populations against changing climatic variability. *Ecology*, **89**, 19–25.

724 Morrison SF, Hik DS (2007) Demographic analysis of a declining pika ochotona
725 collaris population: linking survival to broad-scale climate patterns via spring
726 snowmelt patterns. *Journal of Animal ecology*, **76**, 899–907.

727 Nobel PS (1984) Extreme temperatures and thermal tolerances for seedlings of
728 desert succulents. *Oecologia*, **62**, 310–317.

729 Notaro M, Gutzler D (2012) Simulated impact of vegetation on climate across the
730 north american monsoon region in ccs3. 5. *Climate dynamics*, **38**, 795–814.

- 731 Ogle K, Barber JJ, Barron-Gafford GA, *et al.* (2015) Quantifying ecological mem-
732 ory in plant and ecosystem processes. *Ecology letters*, **18**, 221–235.
- 733 Ohm JR, Miller TE (2014) Balancing anti-herbivore benefits and anti-pollinator
734 costs of defensive mutualists. *Ecology*, **95**, 2924–2935.
- 735 Peters DP, Havstad KM, Archer SR, Sala OE (2015) Beyond desertification: new
736 paradigms for dryland landscapes. *Frontiers in Ecology and the Environment*,
737 **13**, 4–12.
- 738 Petrie M, Collins S, Gutzler D, Moore D (2014) Regional trends and local variabil-
739 ity in monsoon precipitation in the northern chihuahuan desert, usa. *Journal of*
740 *arid environments*, **103**, 63–70.
- 741 Pfister CA (1998) Patterns of variance in stage-structured populations: evolution-
742 ary predictions and ecological implications. *Proceedings of the National Academy*
743 *of Sciences*, **95**, 213–218.
- 744 Plummer M, *et al.* (2003) Jags: A program for analysis of bayesian graphical
745 models using gibbs sampling. In: *Proceedings of the 3rd international workshop*
746 *on distributed statistical computing*, vol. 124. Vienna, Austria.
- 747 Rudgers JA, Chung YA, Maurer GE, Moore DI, Muldavin EH, Litvak ME, Collins
748 SL (2018) Climate sensitivity functions and net primary production: A frame-
749 work for incorporating climate mean and variability. *Ecology*, **99**, 576–582.
- 750 Salguero-Gomez R, Siewert W, Casper BB, Tielbörger K (2012) A demographic
751 approach to study effects of climate change in desert plants. *Philosophical Trans-*
752 *actions of the Royal Society B: Biological Sciences*, **367**, 3100–3114.

- 753 Selwood KE, McGeoch MA, Mac Nally R (2015) The effects of climate change
754 and land-use change on demographic rates and population viability. *Biological*
755 *Reviews*, **90**, 837–853.
- 756 Shriver RK (2016) Quantifying how short-term environmental variation leads to
757 long-term demographic responses to climate change. *Journal of Ecology*, **104**,
758 65–78.
- 759 Sletvold N, Dahlgren JP, Øien DI, Moen A, Ehrlén J (2013) Climate warming alters
760 effects of management on population viability of threatened species: results from
761 a 30-year experimental study on a rare orchid. *Global Change Biology*, **19**, 2729–
762 2738.
- 763 Smith M, Caswell H, Mettler-Cherry P (2005) Stochastic flood and precipitation
764 regimes and the population dynamics of a threatened floodplain plant. *Ecological*
765 *Applications*, **15**, 1036–1052.
- 766 Su YS, Yajima M (2012) R2jags: A package for running jags from r. *R package*
767 *version 0.03-08*, URL <http://CRAN.R-project.org/package=R2jags>.
- 768 Teller BJ, Adler PB, Edwards CB, Hooker G, Ellner SP (2016) Linking demogra-
769 phy with drivers: climate and competition. *Methods in Ecology and Evolution*,
770 **7**, 171–183.
- 771 Tenhumberg B, Crone EE, Ramula S, Tyre AJ (2018) Time-lagged effects of
772 weather on plant demography: drought and astragalus scaphoides. *Ecology*,
773 **99**, 915–925.

- Urban MC (2015) Accelerating extinction risk from climate change. *Science*, **348**, 571–573.
- Van de Pol M, Vindenes Y, Sæther BE, Engen S, Ens BJ, Oosterbeek K, Tinbergen JM (2010) Effects of climate change and variability on population dynamics in a long-lived shorebird. *Ecology*, **91**, 1192–1204.
- Vellend M, Verheyen K, Jacquemyn H, Kolb A, Van Calster H, Peterken G, Hermy M (2006) Extinction debt of forest plants persists for more than a century following habitat fragmentation. *Ecology*, **87**, 542–548.
- Villellas J, Doak DF, García MB, Morris WF (2015) Demographic compensation among populations: what is it, how does it arise and what are its implications? *Ecology letters*, **18**, 1139–1152.
- Wang T, Hamann A, Spittlehouse D, Carroll C (2016) Locally downscaled and spatially customizable climate data for historical and future periods for north america. *PLoS One*, **11**, e0156720.
- Williams JL, Ellis MM, Bricker MC, Brodie JF, Parsons EW (2011) Distance to stable stage distribution in plant populations and implications for near-term population projections. *Journal of ecology*, **99**, 1171–1178.
- Williams JL, Jacquemyn H, Ochocki BM, Brys R, Miller TE (2015) Life history evolution under climate change and its influence on the population dynamics of a long-lived plant. *Journal of Ecology*, **103**, 798–808.
- Williams JL, Miller TEX, Ellner SP (2012) Avoiding unintentional eviction from integral projection models. *Ecology*, **93**, 2008–2014.

- 796 Winkler DE, Conner JL, Huxman TE, Swann DE (2018) The interaction of drought
797 and habitat explain space–time patterns of establishment in saguaro (*Carnegiea*
798 *gigantea*). *Ecology*, **99**, 621–631.
- 799 Yu K, D’Odorico P, Collins SL, *et al.* (2019) The competitive advantage of a con-
800 stitutive CAM species over a C4 grass species under drought and CO2 enrichment.
801 *Ecosphere*, **10**, e02721.

802 Appendix A: Correspondence between downscaled 803 and locally measured climate variables

804 Correlation of climate values

805 We compared warm- and cool-season values of four climate variables (total pre-
806 cipitation and minimum, mean, and maximum temperature) between two data
807 sources: the SEV-LTER meteorological station nearest our study site (station 50 in
808 the SEV-LTER meteorological network) and downscaled data from ClimateWNA
809 corresponding to the same latitude, longitude, and elevation as station 50. Our
810 goal was to determine how well the downscaled data captured conditions ‘on the
811 ground’ as measured directly by the meteorological station. We compared the
812 years 2001 through 2017, which are the years of overlap between the two data
813 sources.

814 There was moderate to strong agreement between the two data sources (Table
815 A1, Fig. A1, Fig. A2). Temperature extrema were less strongly correlated between
816 the two data sets than temperature means (Fig. A1), which is unsurprising given
817 that extreme values may be sensitive to local micro-environmental conditions that
818 the relatively coarse downscaled data would miss. There was an extreme-cold
819 event in 2011 that was particularly poorly captured by the downscaled data (Fig.
820 A1A). The weakest correlation was that of warm-season maximum temperature
821 (Fig. A1F; Pearson’s $r = 0.41$, $P = 0.11$).

Table A1: Correlations between seasonal climate values measured by an on-site meteorological station versus downscaled data from ClimateWNA corresponding to the same years and location. Correlation values show Pearson correlations and P-values come from t -tests with 14 degrees of freedom.

Season	Variable	Correlation	P-value
Warm	Min temperature	0.59	0.0153
Warm	Mean temperature	0.84	10^{-4}
Warm	Max temperature	0.41	0.1135
Warm	Precipitation	0.49	0.0544
Cool	Min temperature	0.51	0.0622
Cool	Mean temperature	0.94	3.6×10^{-7}
Cool	Max temperature	0.69	0.0069
Cool	Precipitation	0.87	4.6×10^{-5}

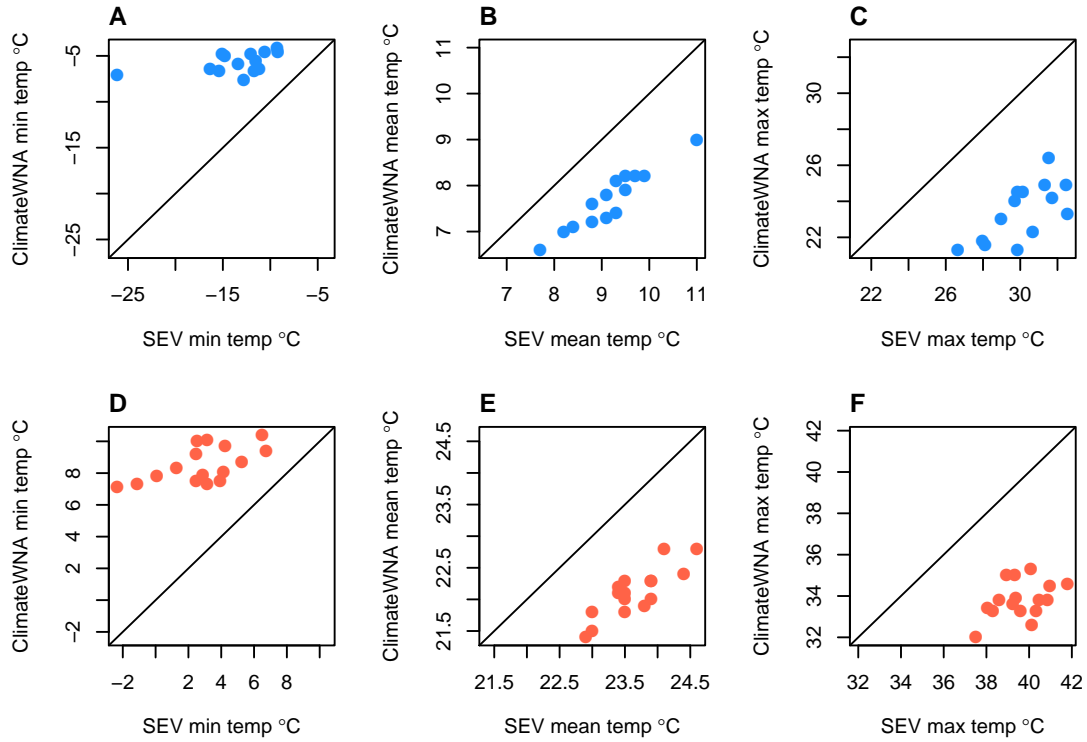


Figure A1: Correlations of minimum, mean, and maximum temperature values of cool (A–C) and warm (D–F) seasons between SEV-LTER meteorological data and downscaled estimates from ClimateWNA for years 2004–2017. Diagonal lines show $y = x$.

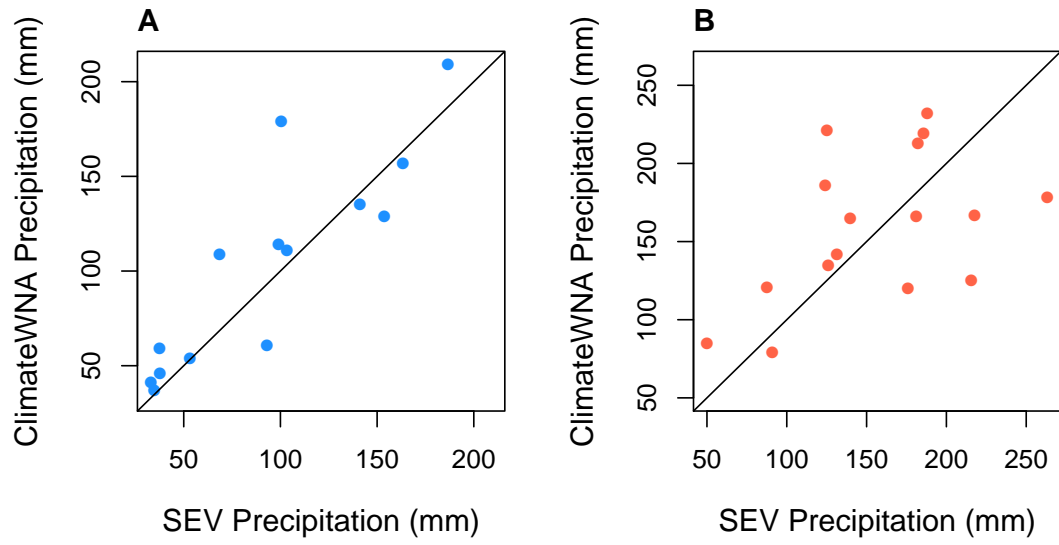


Figure A2: Correlations of cool- (**A**) and warm-season (**B**) precipitation between SEV-LTER meteorological data and downscaled estimates from ClimateWNA for years 2004–2017. Diagonal lines show $y = x$.

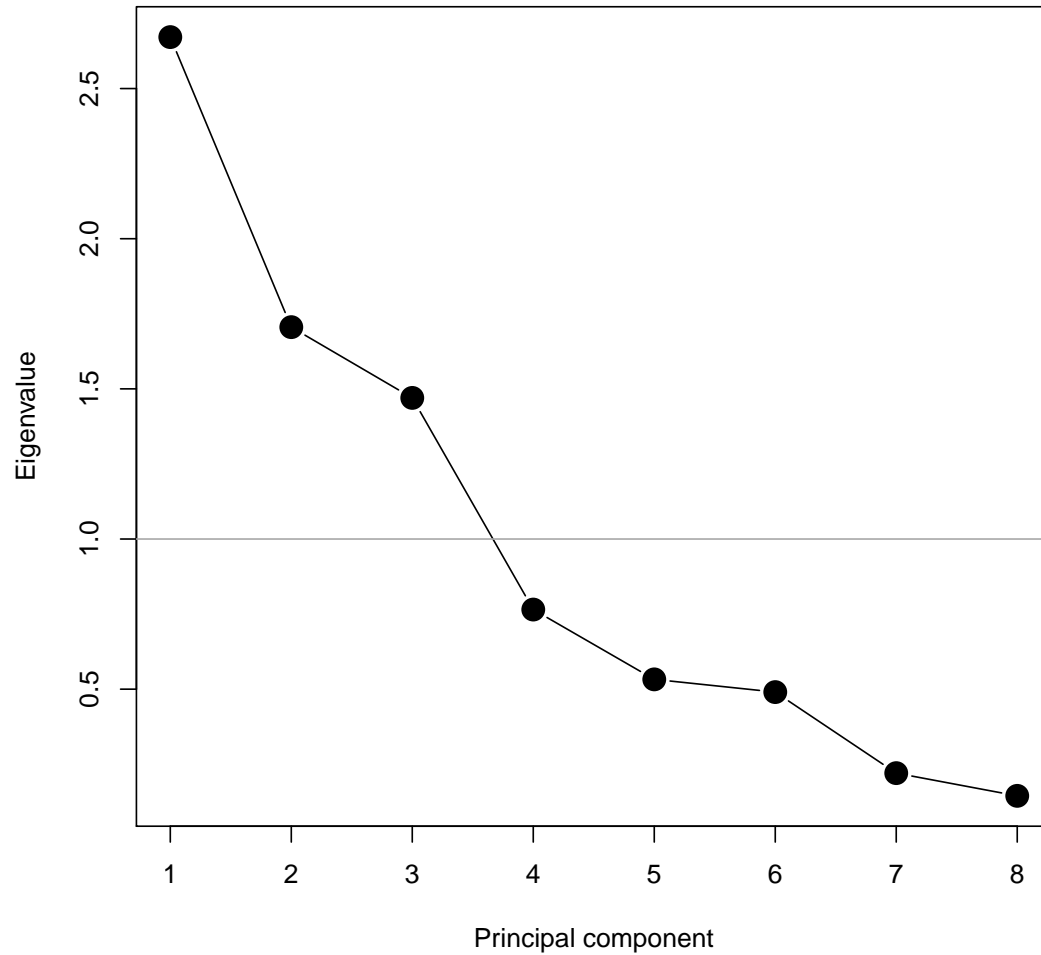


Figure A3: Results of parallel analysis conducted using the R package ‘paran’ (Dinno, 2018). Components with eigenvalues greater than 1 are retained.

822 Re-analysis with SEV-LTER data

823 To further explore the consequences of relying on down-scaled climate data, we
 824 re-ran our demographic analysis using the SEV-LTER meteorological data and

825 compared the results to those based on ClimateWNA. First, we conducted PCA on
826 raw seasonal temperature and precipitation values from SEV Meteorological Sta-
827 tion 50 over the observation years 2004–2017. As in our analysis of ClimateWNA
828 data, parallel analysis supported retention of three principal components. Vari-
829 able loadings onto these PCs are shown in Fig. A4 and show a pattern similar to
830 ClimateWNA data whereby PC1 was dominated by annual differences (cool- and
831 warm-season variables loaded similarly) and PC2-3 were dominated by seasonal
832 climate factors. However, seasonal variable loadings onto PC2 and PC3 were dif-
833 ferent for the two data sets (compare Figs. 1 and A4). Second, we fit the full set
834 of vital rate models to these three PCs and used stochastic variable selection (Ap-
835 pendix B) to eliminate weakly supported climate covariates. When then re-fit the
836 vital rate models including variables with $\hat{z}_i > 0.1$ (see Appendix B). These fitted
837 models are shown in Fig. A5. Note that the PC axes from SEV meteorological
838 data are different PCs than those from ClimateWNA and have different variable
839 loadings. Thus, we expect differences in demographic responses between Figures
840 2 and A5.

841 We compared results based on the two data sources in several ways. First,
842 we compared the inter-annual variances associated with year random effects in
843 the statistical models. We found that, for survival in particular, random variance
844 across years was much lower using SEV-LTER data as climate covariates compared
845 to ClimateWNA (Fig. A6). This tells us that, as expected, on-site data provided
846 greater resolution of climate drivers, since less inter-annual variation in survival
847 was attributed to process error.

848 Second, we used the IPM derived from each data source to generate two pre-
849 dicted time series of climate-sensitive vital rates (survival, flowering, and fertility)

850 and λ during the study years. These time series are shown in Fig. A7. Year-
 851 specific estimates of flowering and fertility showed poor correspondence between
 852 the two data sources (Fig. A7B,C), likely because they were both predicted to
 853 be more responsive to climate in the ClimateWNA analysis (Fig. 2) compared
 854 to the SEV-LTER analysis (Fig. A5). However, year-specific survival rates were
 855 highly consistent between the two data sources (Fig. A7A). Because λ was much
 856 more sensitive to survival than reproduction, year-specific estimates of λ were
 857 also highly consistent and significantly correlated between the two data sources
 858 (Fig. A7D, Fig. A8A; Pearson's $r = 0.59$, $t_{10} = 2.34$, $P < 0.04$). When we
 859 additionally incorporated year-specific random effects estimated from the statis-
 860 tical models, λ estimates were nearly perfectly correlated (Fig. A8B; Pearson's
 861 $r = 0.99$, $t_{10} = 40.36$, $P < 0.0001$). This tight correlation is expected, because
 862 year-specific random effects allow both the SEV-LTER and ClimateWNA models
 863 to match the observations, so it would be a sign of trouble if the relationship in
 864 Fig. A8B was weak. Finally, we found that SEV-LTER climate PCs explained
 865 78% of inter-annual variation in λ , an improvement over the 60% explained by
 866 ClimateWNA PCs.

867 Overall, our re-analysis with SEV-LTER data and comparison between the on-
 868 site SEV and downscaled ClimateWNA data indicates that our qualitative con-
 869 clusions about demography-climate relationships are robust to the choice of data
 870 source. In both analyses, we find vital rate responses to climate that translate to
 871 similar year-specific predictions for population growth rates. However, in relying
 872 on downscaled data for our main analyses, we certainly lost some of the climate
 873 signal. The 18% loss of resolution with ClimateWNA tells us that using down-
 874 scaled data inflated the contribution of process error to our back-casted estimates

875 (Fig. C3A).

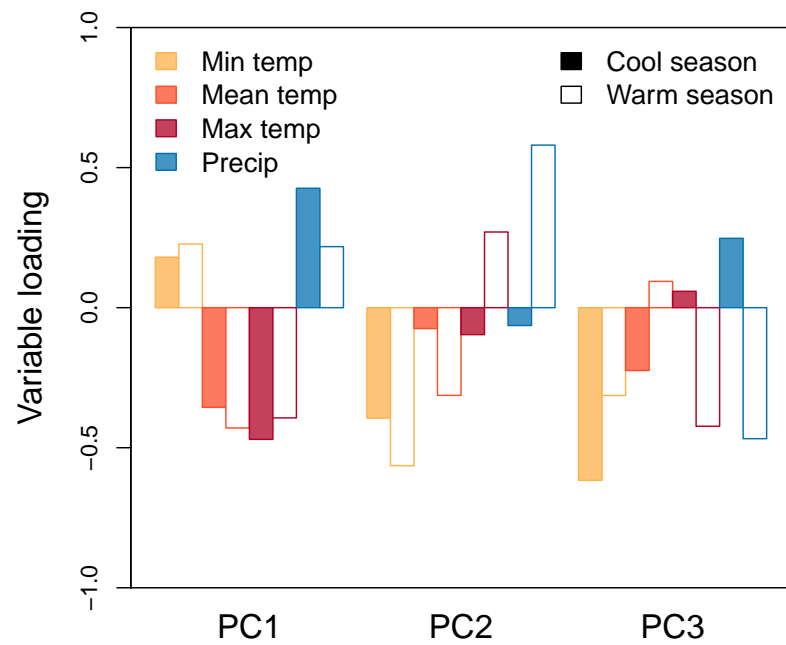


Figure A4: Principal components analysis of SEV-LTER meteorological data. Bars show loadings of raw variables onto three principal components. Layout as in Fig. 1.

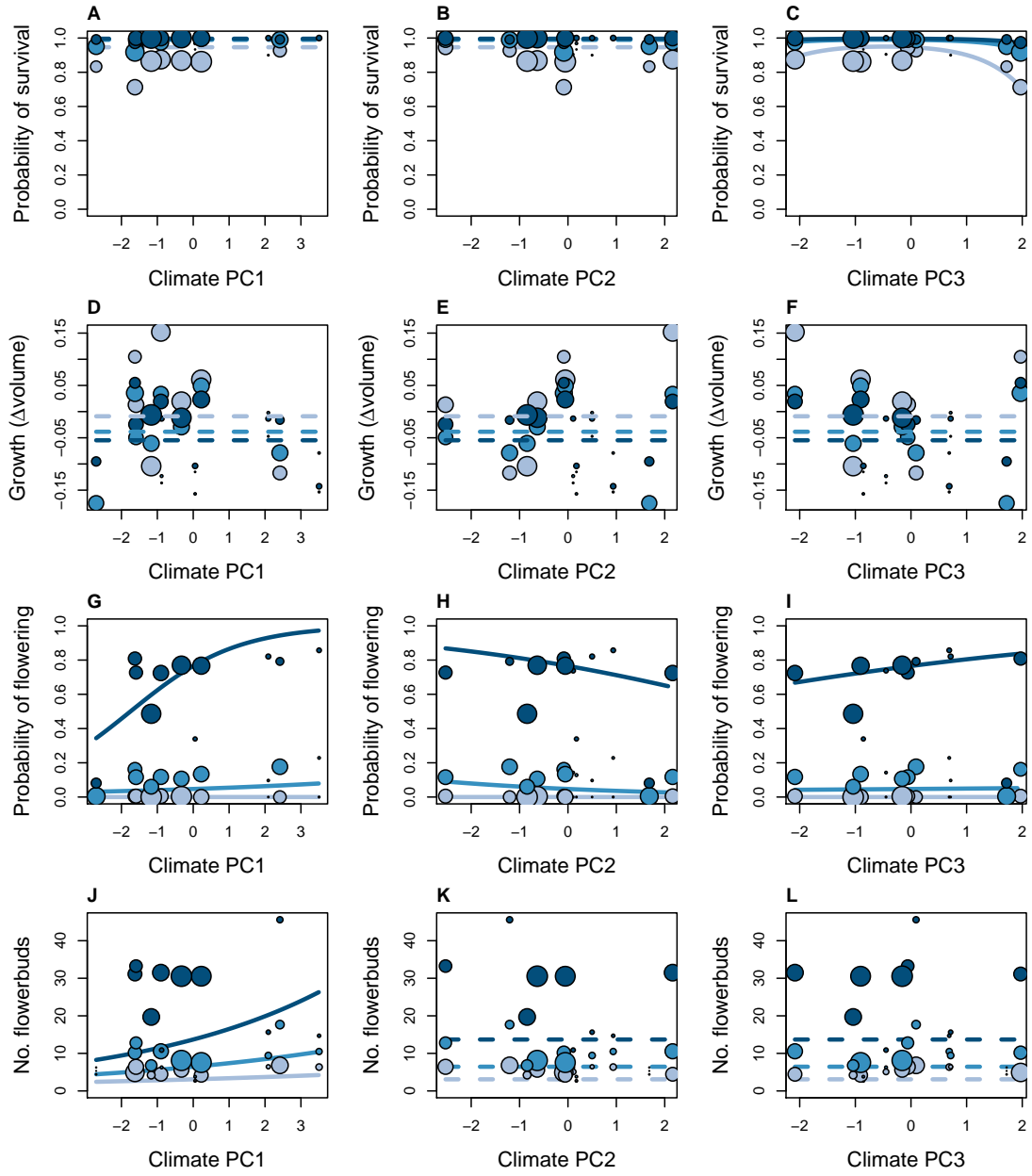


Figure A5: Vital rate data and fitted models using principal components of SEV-LTER meteorological data as climate covariates. Layout as in Fig. 2.

Climate PC	Model term	Survival	Growth	Flowering	Fertility
	Size	1	0.01	1	1
1	PC	0.06	0.01	0.07	0.07
1	PC*PC	0.03	0.01	0.05	0.01
1	PC*size	0.06	0.01	1	0.31
2	PC	0.06	0.01	0.13	0.05
2	PC*PC	0.03	0.01	0.05	0.03
2	PC*size	0.02	0.01	0.04	0.03
3	PC	0.78	0.02	0.09	0.04
3	PC*PC	0.88	0.02	0.08	0.03
3	PC*size	0.04	0.01	0.17	0.02

Table A2: Stochastic variable selection results based on climate data from SEV-LTER. Values (z) can be interpreted as the probability that a model coefficient is non-zero. Bolded values indicate terms retained in the final model.

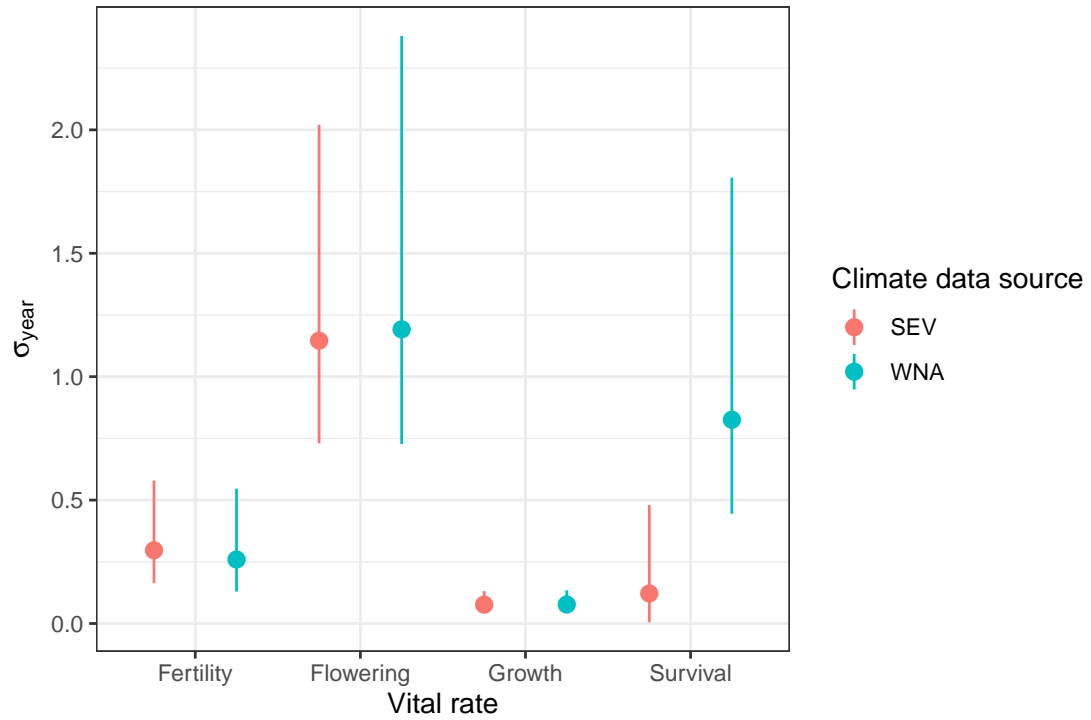


Figure A6: Posterior distributions of inter-annual variance (σ_{year}) associated with year random effects from vital rate models fit with two climate data sources (colors): ClimateWNA and SEV-LTER. Points show posterior means and bars show 95% credible intervals.

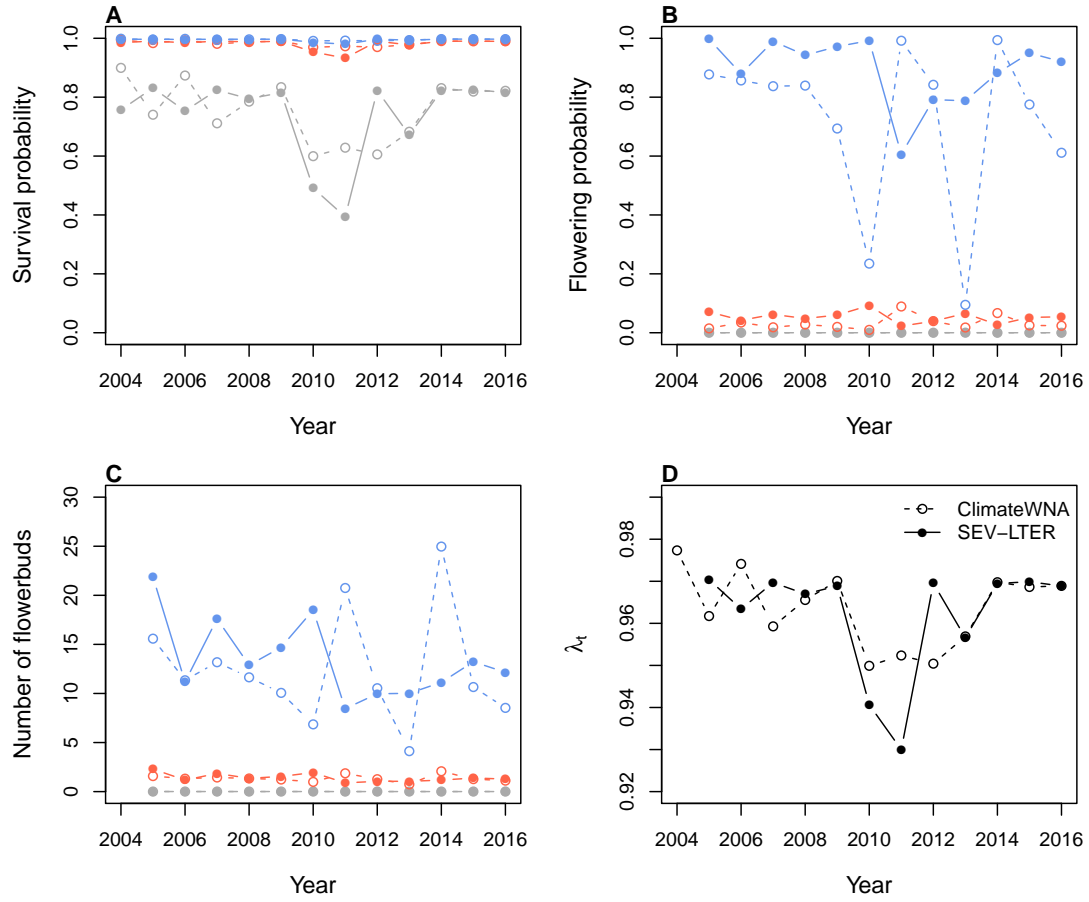


Figure A7: Year-specific estimates of vital rates (A–C) and population growth rates (D) based on SEV-LTER (filled points, solid lines) or ClimateWNA (open points, dashed lines). Climate-dependent vital rates are probability of survival (A), probability of flowering (B), and flowerbud production of flowering plants (C). For each vital rate, colors correspond to three size groups: the 5th (gray), 50th (red), and 95th (blue) percentiles of the size distribution. SEV meteorological data were not available for 2003, so we could not estimate reproductive rates or population growth rates for the 2004 transition year.

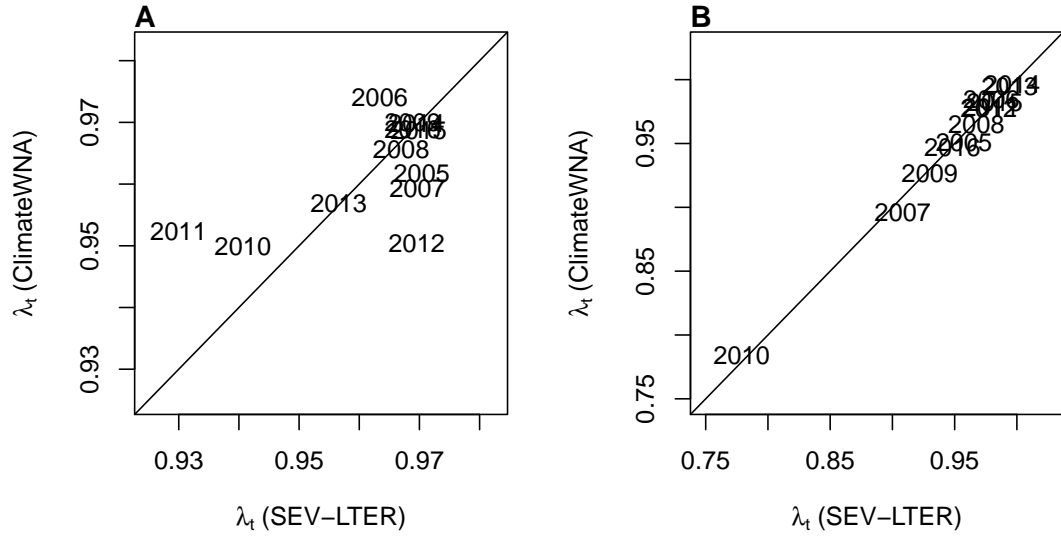


Figure A8: Comparison of year-specific estimates of λ from IPMs using either SEV-LTER (x -axis) or ClimateWNA (y -axis) as climate data sources. Diagonal lines show $y = x$. **A**, λ estimates based only on climate PCs (Pearson's $r = 0.59$, $t_{10} = 2.34$, $P < 0.04$); **B**, λ estimates based on climate and year random effects, which account for inter-annual differences not explained by the climate PCs (Pearson's $r = 0.99$, $t_{10} = 40.36$, $P < 0.0001$).

876 Appendix B: Stochastic variable selection

877 Because we intended to extrapolate the vital rate models into past climate environ-
878 ments that were not well represented during the long-term study, it was important
879 that we simplify the vital rate models to exclude unnecessary coefficients (which,
880 even if small in absolute value, could generate unrealistic predictions when ex-
881 trapolated over a greater range of climate than the models were fitted to). To
882 do this, we used stochastic variable selection, a ‘model-based model selection’
883 approach (Hooten & Hobbs, 2015) that generates weightings for each fixed-effect
884 coefficient, indicating the probability that the coefficient is non-zero. We employed
885 an approach based on George and McCulloch (1993) where each coefficient (C_i)
886 is modeled as a mixture distribution with zero and non-zero modes, where modal
887 frequency is determined by an indicator variable (z_i). The coefficient prior was:

$$C_i \sim (1 - z_i) * N(0, 0.1) + z_i * N(0, 1000) \quad (\text{B1})$$

$$z_i \sim \text{Bernoulli}(0.5) \quad (\text{B2})$$

888 The first term of the mixture distribution assigns, with probability $(1 - z_i)$, a
889 prior with mean zero and arbitrarily small variance, effectively forcing the poste-
890 rior estimate to equal zero. The second term assigns, with probability z_i , a prior
891 with mean zero and arbitrarily large variance, which allows for a non-zero pos-
892 terior estimate. The posterior distribution of the indicator variable z_i gives the
893 probability that the coefficient is non-zero. We estimated this probability for each
894 coefficient in Eq. B1 and retained in the final model all coefficients with a posterior

mean $\hat{z}_i > 0.1$, meaning that the model term is determined to be non-zero with 90% confidence. All z_i values from the full model are shown in Table B1.

Climate PC	Model term	Survival	Growth	Flowering	Fertility
	Size	1	0.53	1	1
1	PC	0.13	0.04	0.12	0.05
1	PC*PC	0.03	0.01	0.03	0.01
1	PC*size	0.06	0.01	0.08	0.07
2	PC	0.18	0.03	0.11	0.14
2	PC*PC	0.06	0.01	0.06	0.03
2	PC*size	0.04	0.02	1	0.27
3	PC	0.18	0.02	0.12	0.18
3	PC*PC	0.09	0.01	0.09	0.06
3	PC*size	0.06	0.01	0.13	0.03

Table B1: Stochastic variable selection results. Values (z) can be interpreted as the probability that a model coefficient is non-zero. Bolded values indicate terms retained in the final model.

897 Appendix C: Additional demographic modeling meth- 898 ods and results

899 We estimated a time series for the stochastic population growth rate (λ_S) over
900 the period 1900-2017 using a moving window approach. While the determinis-
901 tic growth rate for each year estimates the long-run growth rate expected if the
902 conditions of that year remained constant, the stochastic growth rate integrated
903 over a broader range of conditions, incorporating year-to-year fluctuations and
904 auto-correlation of climate variables.

We simulated population dynamics according to Equations 4–2 to estimate the stochastic population growth rate λ_S . We estimated λ_S for 10-year windows spanning the time series 1901–2017, such that the value of λ_S for year t reflects the stochastic growth rate for a climate environment defined by years t through $t + 9$. For each 10-year window, we simulated 1000 years of population dynamics, each year randomly drawing one of the 10 climate-years. For each year of the simulation, we calculated total population size as:

$$N_t = \int n(x)_t dx + B_{1,t} + B_{2,t} \quad (\text{C1})$$

and estimated the stochastic growth rate for that window as the expected value of the one-year growth rate:

$$\log(\lambda_S) = \mathbb{E}[\log(\frac{N_{t+1}}{N_t})] \quad (\text{C2})$$

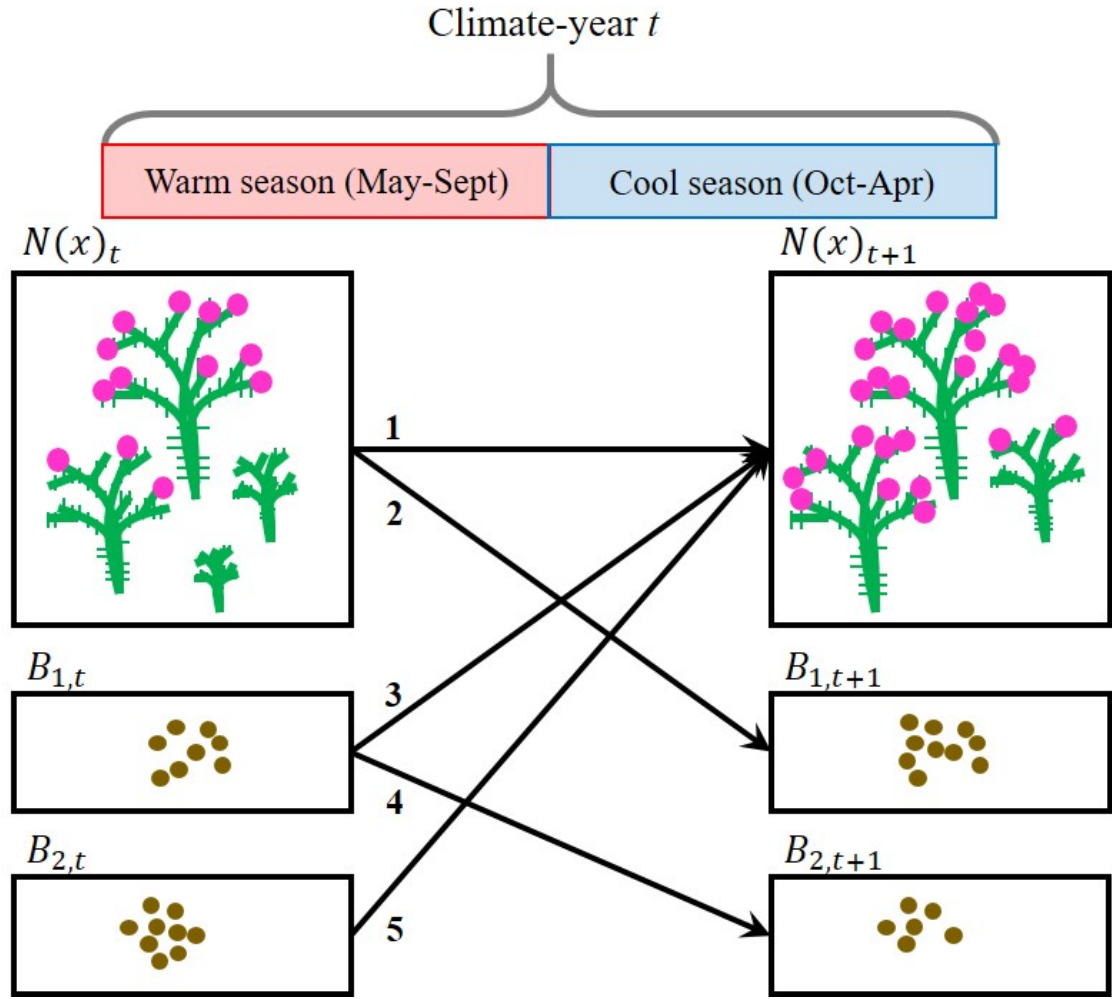


Figure C1: *C. imbricata* life cycle and census timing with respect to warm- and cool-season climate. Numbered arrows correspond to demographic events that occur during a transition year: (1) established plants survive and grow, (2) plants that are reproductive in year t contribute seeds that will make up the 1-yo seed bank in year $t+1$, (3) a fraction of seeds in the 1-yo seed bank survive and recruit into the plant population as seedlings in year $t+1$, (4) another fraction of seeds in the 1-yo seed bank survives and remains to form the 2-yo seed bank in year $t+1$, (5) a fraction of seeds in the 2-yo seed bank survive and recruit into the plant population as seedlings in year $t+1$. Survival and growth from year t to year $t+1$ (arrow 1) depended on climate year year t , whereas flowering and flowerbud production in year t (components of arrow 2) depended on climate in year $t-1$.

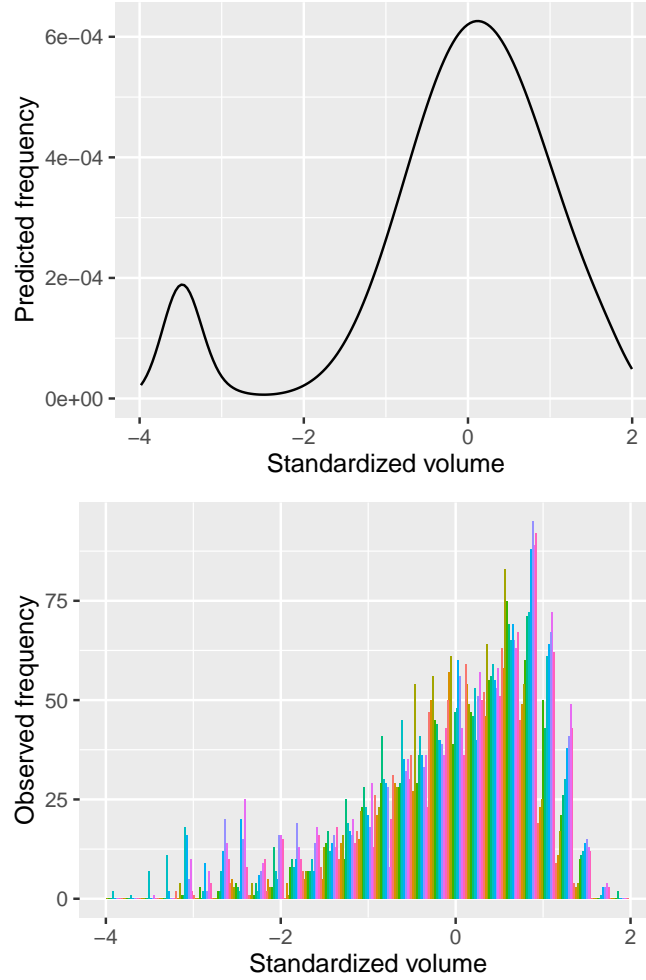


Figure C2: Comparison of predicted (top) and observed (bottom) size distributions, where size was the natural logarithm of plant volume standardized to mean zero. In the bottom panel, different colors represent different years. The predicted stable size distribution (evaluated at the average climate) corresponded well to the observed size distribution, though very large plants were over-represented in the observed distribution. This is consistent with the idea that the population may have recently transitioned into decline, whereby the persistence of large plants may reflect a legacy of positive growth rates. Also, the peak for new recruits was at a larger size in the observed distribution, but this was likely a consequence of the fact that we rarely detected new recruits. The “new” plants in our plots each year were likely several years old.

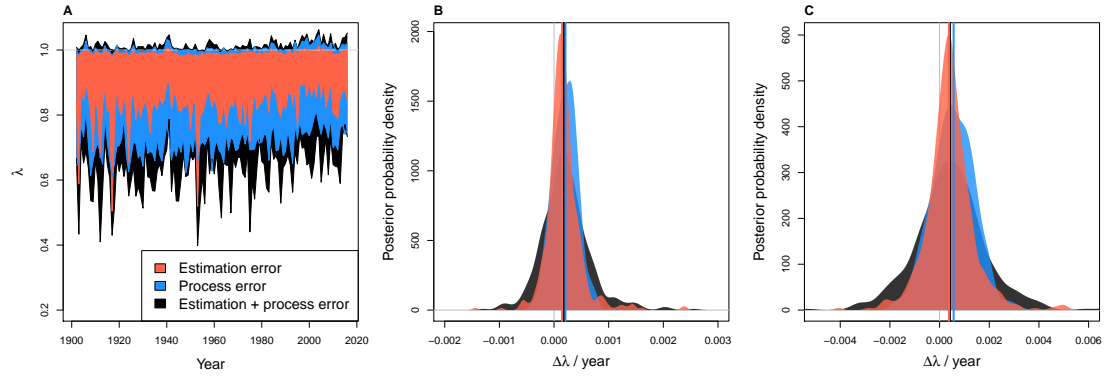


Figure C3: **A**, Time series of back-casted asymptotic population growth rates (λ) predicted based on inter-annual variation in three climate PCs. Shaded regions show the 95% credible interval of the posterior probability distributions for three uncertainty scenarios: estimation error only (parameter uncertainty; red), process error only (year-to-year heterogeneity unrelated to the climate PCs; blue), and both estimation and process error (black). **B**, **C**, Posterior probability distribution for the change in λ per year based on the entire time series (**B**) or years since 1970 (**C**). Vertical lines show the medians of the posterior distributions. Colors as in **A**.

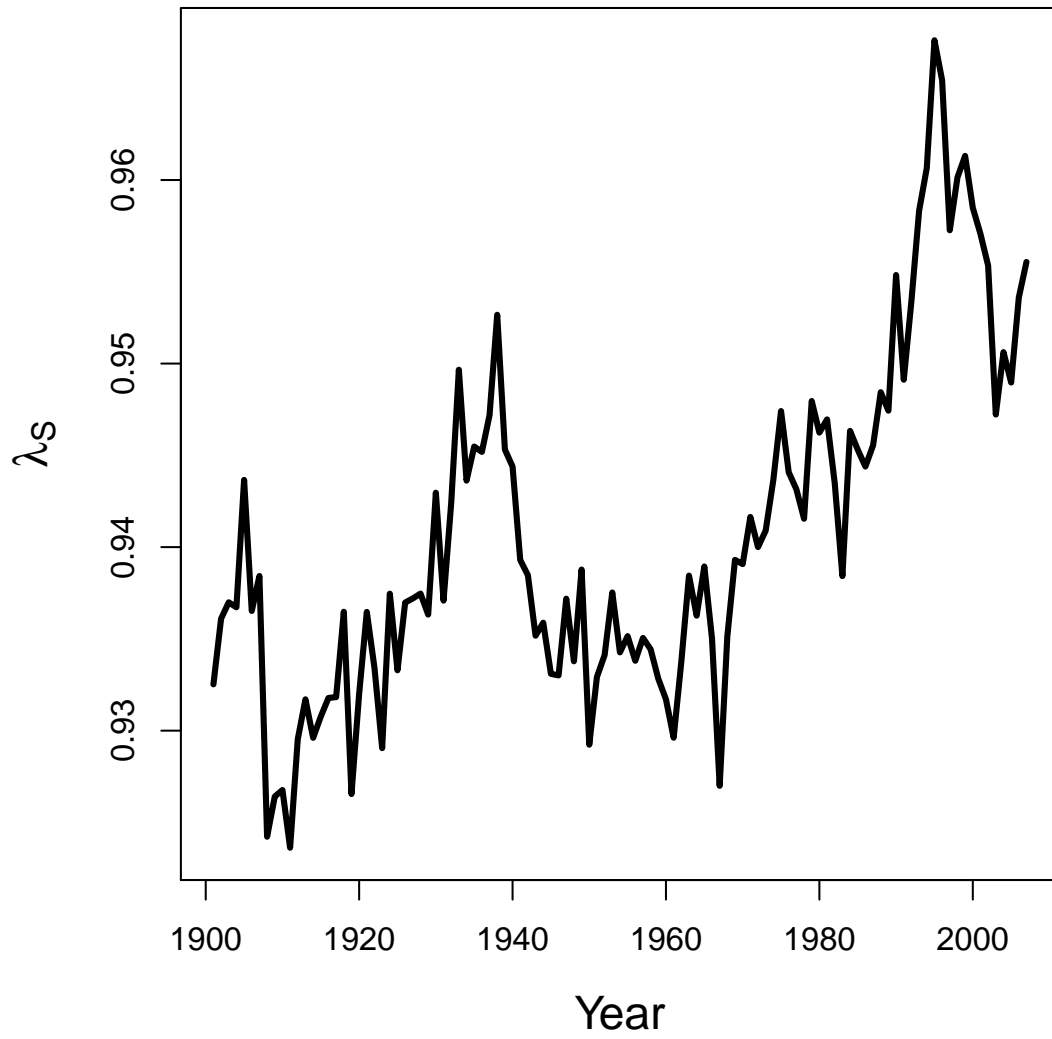


Figure C4: Time series of stochastic population growth rates (λ_S). Values are based on a 10-year sliding window such that λ_S is year t is based on the climate regime over the years t through $t + 9$

905 Appendix D: Exploring the consequences of climate 906 extrapolation

907 Our analysis in the main text relied on extrapolating demographic responses to
908 climate into climate environments that were not directly observed during our field
909 study. For example, high values of PC1 and low values of PC2 were under-
910 represented during the study years (Fig. D1). We explored the consequences
911 of this extrapolation by re-running our demographic analysis with bounds on cli-
912 mate responses. For each vital rate that responded to a climate PC according to
913 some function $f(PC)$, we defined a second function $f^*(PC)$ as:

$$f^*(PC) = \begin{cases} f(PC_L), & \text{if } PC < PC_L \\ f(PC_U), & \text{if } PC > PC_U \\ f(PC), & \text{otherwise} \end{cases} \quad (\text{D1})$$

914 where PC_L and PC_U are the lower and upper bounds, respectively, of the observed
915 range of PC values. For simulations into historical climates more extreme than
916 observed, this approach pins demographic responses to equal the responses at
917 observed extrema, as can be seen in λ responses to PC variation (Fig. D2). We
918 repeated our back-casting analysis using this approach.

919 Results show that our qualitative results are not affected by climate extrapola-
920 tion. The back-casted time series of λ was generally consistent with and without
921 extrapolation (Fig. D3). The main differences were in the extreme low λ values,
922 which were lower with extrapolation. Both time series yielded a positive temporal
923 trend, though the mean change in λ per year was 35% weaker for the entire time

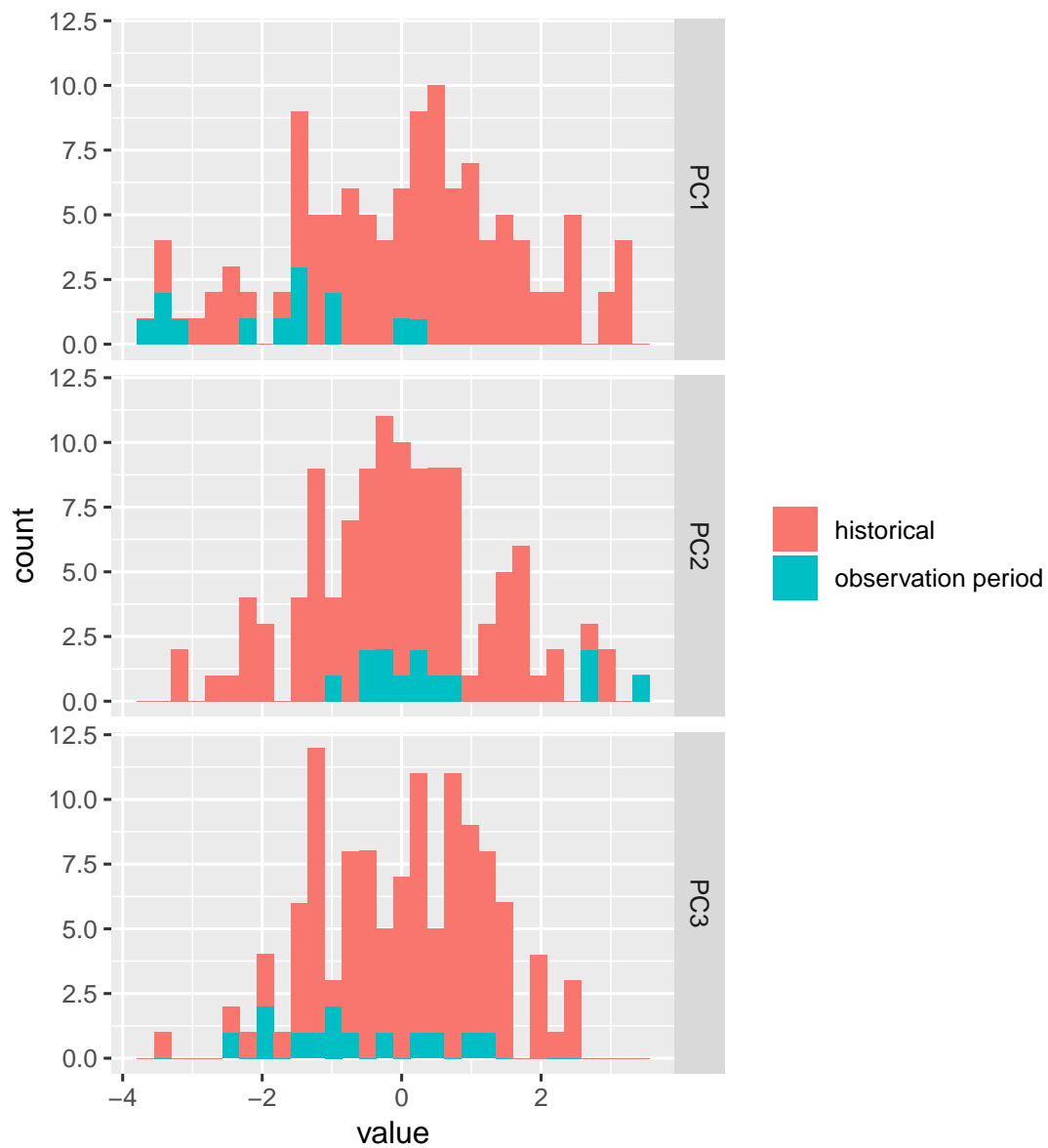


Figure D1: Distributions of observed climate values during the observation period (2004–2017) relative to historical values (1901–2016). Climate values are three principal components of inter-annual variation in cool- and warm-season temperature and precipitation.

series and 26% weaker since 1970 when vital rates were not extrapolated (Fig.
D2). The limited influence of extrapolation was due to the fact that we relied

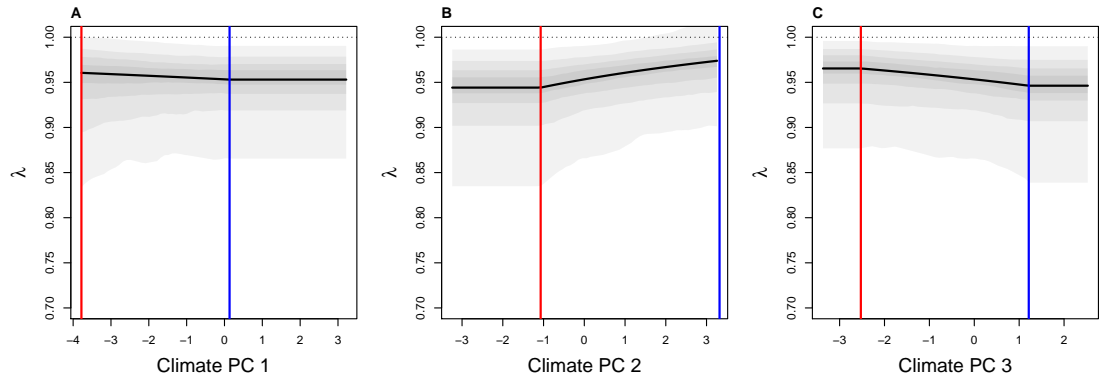


Figure D2: Relationships between λ and three climate PCs with no extrapolation into unobserved climate conditions. For PC values lower than the minimum (red vertical lines) and greater than the maximum (blue vertical lines) of the observation period, demographic responses were forced to match the extrema of the observation period according to Eq. D1.

926 most heavily on extrapolation for PC1 (Fig. D1). As we show in the main paper,
 927 this PC has changed the most during the historical record but it had the weakest
 928 effects on cactus demography.

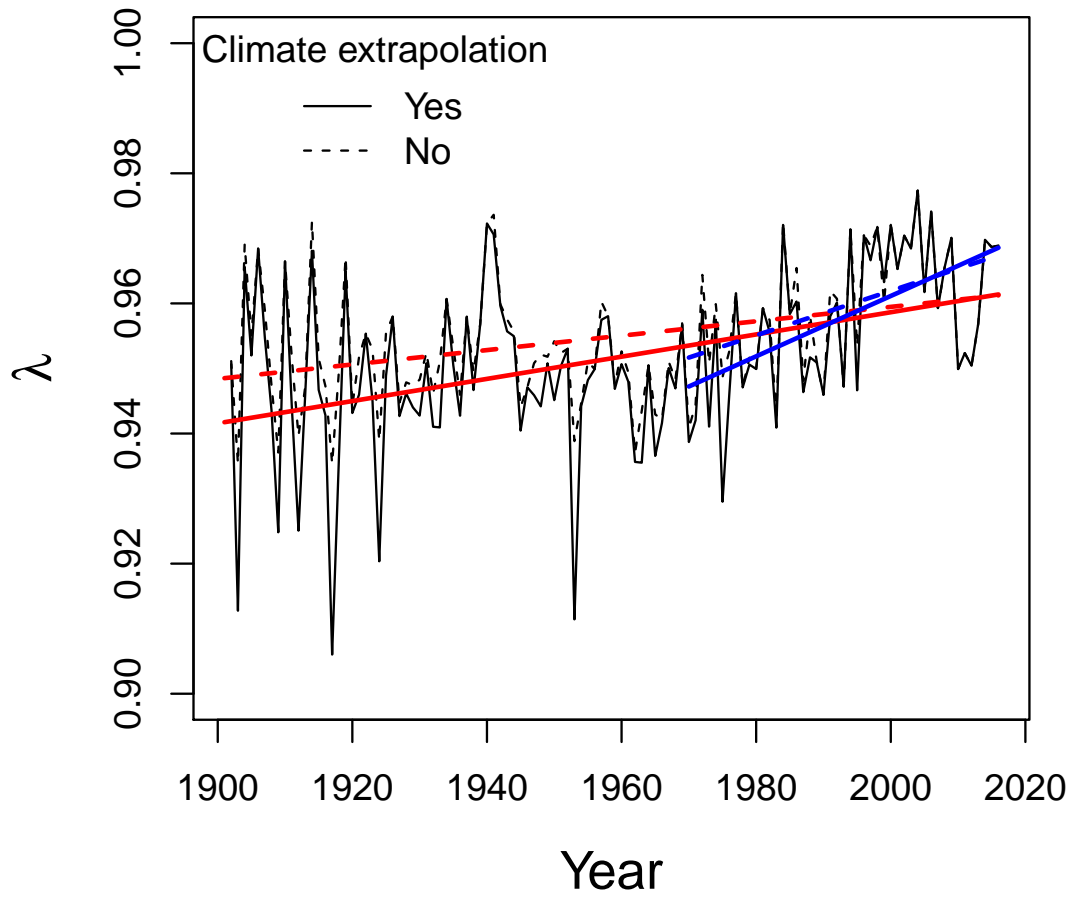


Figure D3: Back-casted values of climate-dependent population growth (λ) with (solid lines) and without (dashed lines) extrapolation of vital rate responses to unobserved climate conditions based on posterior mean parameter values. Red and blue lines show fitted regressions for the entire time series and since 1970, respectively.

Table C1: Parameter values of tree cholla IPM.

Parameter description	Symbol	Mean	95%CI
Survival coefficients	β_0	3.33	(1.4 – 5.25)
	β_1	1.31	(1.18 – 1.44)
	ρ_1^1	-0.11	(-0.82 – 0.61)
	ρ_1^2	0.41	(-0.25 – 1.13)
	ρ_1^3	-0.28	(-0.84 – 0.3)
Survival year variance	σ_{year}	0.9	(0.44 – 1.81)
Survival plot variance	σ_{plot}	0.2	(0.01 – 0.51)
Growth coefficients	β_0	-0.03	(-0.08 – 0.02)
	β_1	-0.02	(-0.03 – -0.02)
Growth residual variance	σ	0.25	(0.25 – 0.26)
Growth year variance	σ_{year}	0.08	(0.05 – 0.13)
Growth plot variance	σ_{year}	0.02	(0.01 – 0.04)
Flowering coefficients	β_0	-4.76	(-7.37 – -2.22)
	β_1	5.17	(4.78 – 5.54)
	ρ_1^1	-0.26	(-1.27 – 0.7)
	ρ_1^2	0.07	(-0.85 – 1.01)
	ρ_3^2	1.11	(0.65 – 1.61)
	ρ_1^3	-0.04	(-0.79 – 0.77)
Flowering year variance	ρ_3^3	0.21	(-0.06 – 0.47)
	σ_{year}	1.28	(0.73 – 2.38)
Flowering plot variance	σ_{year}	0.41	(0.22 – 0.74)
Fertility coefficients	β_0	-0.25	(-0.6 – 0.1)
	β_1	2.22	(2.01 – 2.42)
	ρ_1^2	0.06	(-0.15 – 0.28)
	ρ_3^2	0.17	(-0.01 – 0.35)
	ρ_1^3	0.12	(-0.04 – 0.29)
Fertility year variance	σ_{year}	0.28	(0.13 – 0.55)
Fertility plot variance	σ_{year}	0.31	(0.18 – 0.53)
Seeds per fruit	κ	113.46	(93.47 – 132.59)
Recruitment into seed bank	δ	0.03	(0.02 – 0.05)
Germination rates	γ_1	0.0059	(0.0047 – 0.0073)
	γ_2	0.0044	(0.0033 – 0.0056)
Seedling size distribution	μ_s	-3.49	(-3.62 – -3.37)
	σ_s	0.23	(0.15 – 0.35)
Seedling survival	ω	0.5	(0.002 – 0.998)
Size bounds	L	-3.94	
	U	1.89	